



TALLINNA TEHNICAÜLIKOO
INSENERITEADUSKOND
Ehituse ja arhitektuuri instituut

PUIDUST I-TALADE SÖESTUMISE ULATUSE ANALÜÜS STANDARDTULEKAHJUOLUKORRAS

CHARRING ANALYSIS OF WOODEN I-JOISTS IN STANDARD FIRE

MAGISTRITÖÖ

Üliõpilane: **Hugo Manguse**

Üliõpilaskood: 153854EAEI

Juhendaja: Prof. Alar Just
Kaasjuhendaja: Katrin Nele Mäger

(Tiitellehe pöördel)

AUTORIDEKLARATSIOON

Olen koostanud lõputöö iseseisvalt.

Lõputöö alusel ei ole varem kutse- või teaduskraadi või inseneridiplomit taotletud. Kõik töö koostamisel kasutatud teiste autorite tööd, olulised seisukohad, kirjandusallikatest ja mujalt pärinevad andmed on viidatud.

“.....” 2020

Autor:

/ allkiri /

Töö vastab bakalaureusetöö/magistritööle esitatud nõuetele

“.....” 2020

Juhendaja:

/ allkiri /

Kaitsmisele lubatud

“.....”2020

Kaitsmiskomisjoni esimees

/ nimi ja allkiri /

Lihtlitsents lõputöö reprodutseerimiseks ja lõputöö üldsusele kättesaadavaks tegemiseks¹

Mina _____ (autori nimi) (sünnikuupäev:)

1. Annan Tallinna Tehnikaülikoolile tasuta loa (lihtlitsentsi) enda loodud teose

(lõputöö pealkiri)

mille juhendaja on

(juhendaja nimi)

1.1 reprodutseerimiseks lõputöö säilitamise ja elektroonse avaldamise eesmärgil, sh Tallinna Tehnikaülikooli raamatukogu digikogusse lisamise eesmärgil kuni autoriõiguse kehtivuse tähtaja lõppemiseni;

1.2 üldsusele kättesaadavaks tegemiseks Tallinna Tehnikaülikooli veebikeskkonna kaudu, sealhulgas Tallinna Tehnikaülikooli raamatukogu digikogu kaudu kuni autoriõiguse kehtivuse tähtaja lõppemiseni.

2. Olen teadlik, et käesoleva lihtlitsentsi punktis 1 nimetatud õigused jäävad alles ka autorile.

3. Kinnitan, et lihtlitsentsi andmisega ei rikuta teiste isikute intellektuaalomandi ega isikuandmete kaitse seadusest ning muudest õigusaktidest tulenevaid õigusi.

¹Lihtlitsents ei kehti juurdepääsupiirangu kehtivuse ajal, välja arvatud ülikooli õigus lõputööd reprodutseerida üksnes säilitamise eesmärgil.

_____ (allkiri)

_____ (kuupäev)

TalTech Ehituse ja arhitektuuri instituut

LÕPUTÖÖ ÜLESANNE

Üliõpilane: Hugo Manguse, 153854EAEI

Õppekava, peeriala: EAEI02/09, Ehitiste projekteerimine ja ehitusjuhtumine

Juhendaja(d): Prof Alar Just,
Katrín Nele Mäger

Konsultant:

Lõputöö teema:

Analysis of charring scenarios of wooden I-joists

Lõputöö põhieesmärgid:

- 1.
- 2.
- 3.

Lõputöö etapid ja ajakava:

Nr	Ülesande kirjeldus	Tähtaeg
1.	Kirjanduse ülevaade	
2.	Katseandmete analüüs (katseandmed juhendaja poolt)	
3.	Tulekatsed I-taladega	
4.	Katseandmete analüüs	
5.	Tegurite määramine söestumise arvutusmudeli jaoks	

Töö keel: Inglise

Lõputöö esitamise tähtaeg: "26" mai 2020.a

Üliõpilane: Hugo Manguse ".....".....202....a
/allkiri/

Juhendaja: Alar Just ".....".....202....a

Katrín Nele Mäger ".....".....202....a

/allkiri/

/allkiri/

Kinnise kaitsmise ja/või lõputöö avalikustamise piirangu tingimused formuleeritakse pöördel

Contents

1	Introduction.....	5
2	Fire safety	7
2.1	Fire resistance	8
2.2	Burning of wood.....	8
2.3	Timber frame assemblies	10
2.4	Effect of protection layers.....	11
2.5	Effect of cavity insulation	13
2.6	Improved design model for timber frame assemblies	14
3	Timber frame assemblies with I-shaped members	17
3.1	I-joists.....	17
3.2	Fire design model.....	19
4	Model scale fire tests	20
4.1	April 2019 model scale fire test.....	22
4.1.1	Test specimen	22
4.1.2	Test description	30
4.1.3	Test results	32
4.2	December 2019 model scale fire test	40
4.2.1	Test specimen	40
4.2.2	Test description	42
4.2.3	Test results	43
5	Analysis	46
5.1	Start time of charring and fall-off times.....	46
5.2	Charring rate	47
5.3	Recession speed.....	51
5.4	Residual cross-sections	54
5.5	Cross-section factor.....	57
5.6	Post-protection factor	59
6	Comparison	62
7	Conclusion.....	66
8	Resümee	67
9	References	68

1 Introduction

Wood has been used as a construction material for centuries. It is still a preferred material for constructing smaller residential houses due to its versatility and aesthetics. However, during the last century, wood has somewhat been replaced with newer materials - steel, concrete and cement-based masonry. One of the many reasons for the replacement of wood in construction is fire safety requirements. Wood is considered to be combustible, however, it takes a substantial amount of heat to make it ignite. With proper fire protection, wood is a considerable competitor for more conventional buildings.

The development of wood technology has provided the construction industry with many innovative methods and new products. One of the eminent creations is engineered lumber, such as I-beams. They have three main parts – upper flange, lower flange and a web between them. The web is commonly made of OSB or plywood while the flanges are solid timber or laminated veneer lumber (LVL). Both of the flanges and the web can be jointed to make longer spans otherwise impractical with sawn timber.

I-joists have become more relevant in residential framing and are used extensively in floor, roof and wall framing. They are gradually replacing traditional dimensional timber due to their great strength-to-weight ratio. In addition, I-beams are constructed under strict quality control with low moisture content, thereby diminishing the effects of shrinking. Due to their lightweight, I-beams are easy to install at the construction site and are ideal for longer spans. They don't need heavy-lifting cranes to be installed therefore further lowering their carbon footprint.

Constructions made of I-joists are more sensitive to direct fire as they burn quicker and lose their structural integrity faster when exposed to direct fire than constructions made of dimensional lumber. Therefore, it is crucial to understand how I-beams perform in fire so designers have trustworthy and certified guidelines to design safer buildings.

Aim of the thesis

The main aim of this thesis is to propose new expressions for the cross-section and protection factors for the new model for the fire design of I-joists. The new model is to be added to the new version of the European design standard for timber structures EN 1995-1-2.

Acknowledgments

I take this opportunity to express my heartiest gratitude to people and institutions who have contributed to making this thesis possible.

Foremost, my supervisor, Alar just who introduced me to the world of fire safety and fire testing. I thank him for suggesting the topic of this thesis and for providing me valuable guidance in the process of making my thesis.

My deep gratitude goes to my co-supervisor Katrin Nele Mäger. This thesis would not have been possible without her. I thank her for giving me thoughtful feedback and encouragement to keep on writing. It has been a great honour to work under their supervision.

It is a great pleasure to acknowledge my deepest thanks to Masonite Beams for their support that benefited this study. Most especially, I would like to thank Tommy Persson, Mantas Dovidavicius, and Alfred Wikner.

I am very grateful for the opportunity to attend Forum Wood Building Baltic 2019 conference and for a chance to visit Sweden and Norway as part of this study. I would like to thank all the people whom I met during the conference and during the travel.

Above ground, I am thankful for my family and all the friends for supporting me throughout my studies.

2 Fire safety

Fire safety of buildings as a concept is comprised of a wide array of factors – the design, materials, building practices, occupancy, fire detection and fighting strategies, etc. The responsibility of the structural engineer is to design the load-bearing and separating structures according to the appropriate regulation. According to European Construction Products regulation No 305/2011 [1], construction works must be designed in such a way that in the event of fire:

- the load-bearing capacity of the construction can be assumed for a specific period of time,
- the generation and spread of fire and smoke within the works are limited,
- the spread of the fire to neighbouring construction works is limited,
- the safety of rescue teams is taken into consideration.

The specified requirements for building are stated in national regulations. Eurocodes are a harmonised system of structural design standards. They provide common design methods, which are intended to be used as reference documents for member states to determine the performance of structural components and kits with regard to mechanical resistance and stability and resistance to fire, insofar as it is part of the information accompanying CE marking. The structural fire design of timber structures is specified in EN 1995-1-2 [2].

Fire development in a compartment can be characterized in four stages: incipient, growth, fully developed and decay (see Figure 2.1). Flashover is not considered to be a stage, rather a point in time where there is a sudden spread of flame, where all combustible materials ignite. Fire resistance is effective in the fully developed fire. [3]

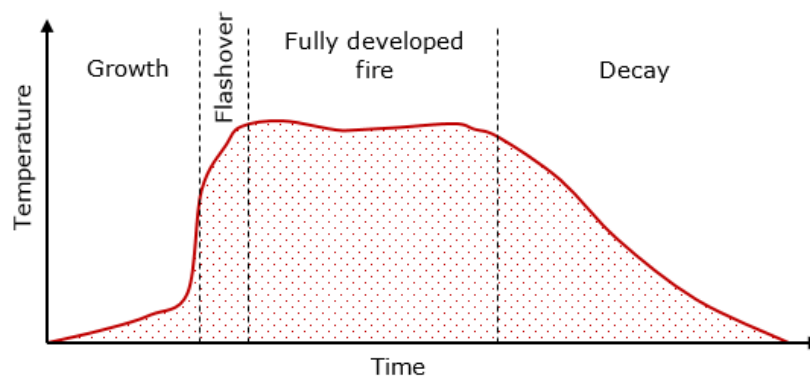


Figure 2.1 Fire development in compartment

2.1 Fire resistance

Structural elements shall withstand a fully developed fire and fulfil requirements of insulation, integrity and/or load-bearing. The fire resistance of timber structures can be determined by calculations according to Eurocode 5 Part 1-2 [4] or by testing e.g. according to EN 13501-2:2009 [5].

The fire resistance is determined as time in minutes in which the structure reaches their failure point when exposed to the standard fire test. The performance criteria are load-bearing (R), integrity (E) and Insulation (I), combined with a time value in minutes. Essentially, the main point of fire safety is always the health and safety of people. The principal cause of death in a fire is carbon dioxide poisoning while the heat is considered to be a primary reason for damages to the structure. [6]

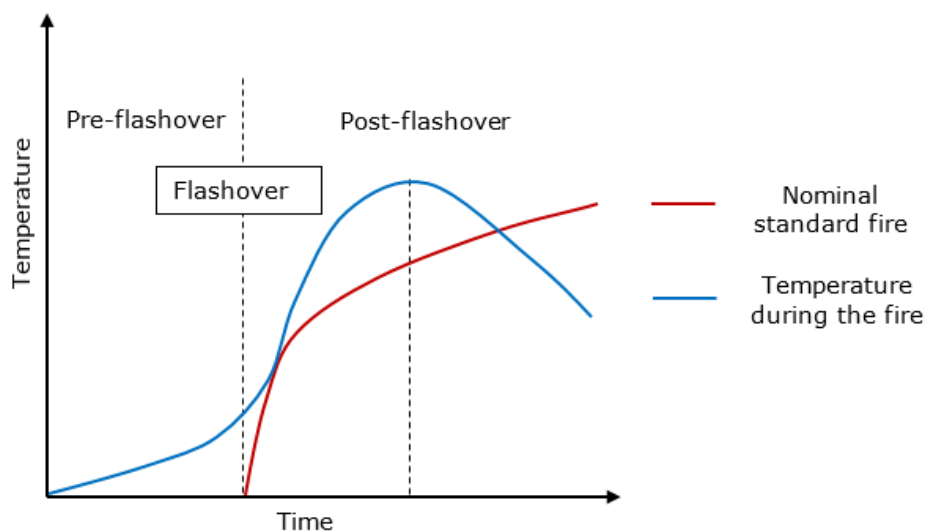


Figure 2.1-1 Nominal standard fire curve nominal standard fire curve

2.2 Burning of wood

Burning of wood is a complex chemical reaction where combustion occurs between the gases released from wood at higher temperatures and oxygen. Ignition and combustion of wood are based on thermal decomposition of cellulose. Ignition of wood begins at 300°C subsequently, a carbon layer is formed on the exposed side of the wood which protects unaffected wood from the heat (see Figure 2.2-1). [4]

Charring is applicable in any direction that means that there is no differentiation for vertical or horizontal charring as the pyrolysis front always proceeds into the wood. Charring rate is a fundamental parameter for fire safety. [6]

Charring of timber is categorised:

1. One dimensional charring, where the charring rate is affected by physical properties (e.g. wood species);
2. Two-dimensional charring, where the charring rate is affected by physical properties and the dimensions of the cross-section.

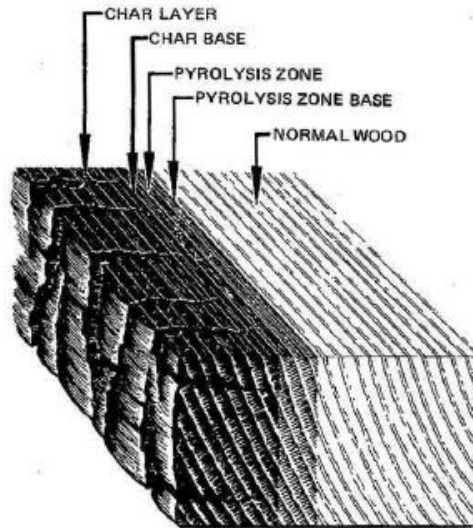


Figure 2.2-1 - Different phases of burning wood [7]

As a basic value, the one-dimensional charring rate β_0 is the rate observed for one-dimensional heat transfer under nominal standard fire of directly exposed fire. Charring can be considered one-dimensional when considering with a semi-infinite slab and no joints or gaps are present. Charring depth is the distance between the outer surface of the original member and position of the char-line. According to EN 1995-1-2 [4], the design charring depth is expressed as:

$$d_{char,0} = \beta_0 \cdot t \quad (1)$$

Where t is time of the exposure and β_0 is one-dimensional design charring rate under standard fire exposure perpendicular to the grain (see Figure 2.2-2). [4]

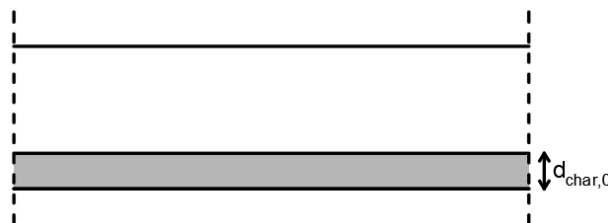


Figure 2.2-2 - One-dimensional charring

When an element with a rectangular cross-section is burning the heat flux is generally two-dimensional near the corners, resulting in a rounded shape of the leftover cross-section. Since the calculation of the residual rounded cross-section is very complicated then an

equivalent rectangular cross section is used, replacing the one-dimensional charring depth and rounding with a notional charring depth (see Figure 2.2-3).

The notional charring depth should be expressed as:

$$d_{char,n} = \beta_n \cdot t \tag{2}$$

where β_n is notional charring rate and t is the time of the exposure. Most used charring rates are listed in Table 2-1. [4]

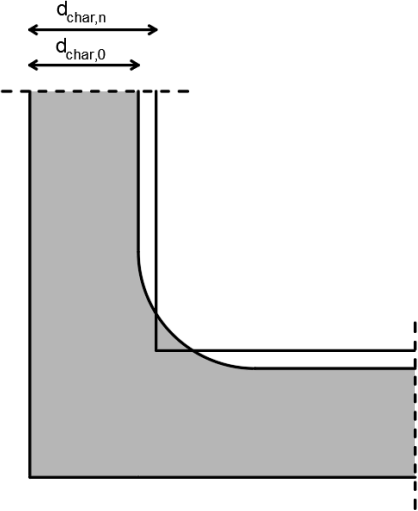


Figure 2.2-3 - One-dimensional charring depth $d_{char,0}$ and notional charring depth $d_{char,n}$

Table 2-1 Charring rate observed for one-dimensional heating [4]

Softwood and beeches	β_0
Glued laminated timber with a characteristic density of $\geq 250 \text{ kg/m}^3$	0.65
Solid timber with a characteristic density of $\geq 290 \text{ kg/m}^3$	0.65

2.3 Timber frame assemblies

One of the most widely used wooden load-bearing structure that is either made from I-joists or solid wood are titled as timber frame assemblies (TFA) which are designed to erect all structural elements such as walls and floors. The materials commonly used in a timber frame system are wooden studs that are sheathed on the exterior side with wood-base boards such as plywood or OSB. On the interior mineral-based boards are used that provide support for a surface finish. The wooden panels on the exterior side give racking resistance to the whole element. The cavities may be void or completely filled with a wide range of insulations. The function of mass insulation is to reduce noise and to control the temperature of inside surfaces that affect the comfort of occupants and aid or deter

condensation. Multiple layers of insulations could be placed with the help of braces. The TFA can be manufactured on-site or in the factory which shortens the construction timeline. [8]

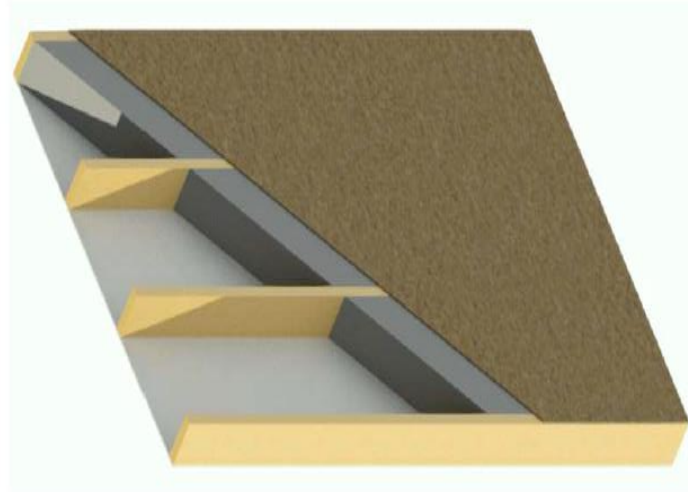


Figure 2.3-1 Timber frame assembly.

2.4 Effect of protection layers

In the case of protected cross-sections the start of charring is delayed. In addition, the development of char also provides protection against the heat flux and the rate of charring is slowed down even more. An adequate char thickness is considered to be 25 mm for it to provide protection for the remaining unburnt residual cross-section. Charring depth and relation to time is illustrated in Figure 2.4-1. [9]

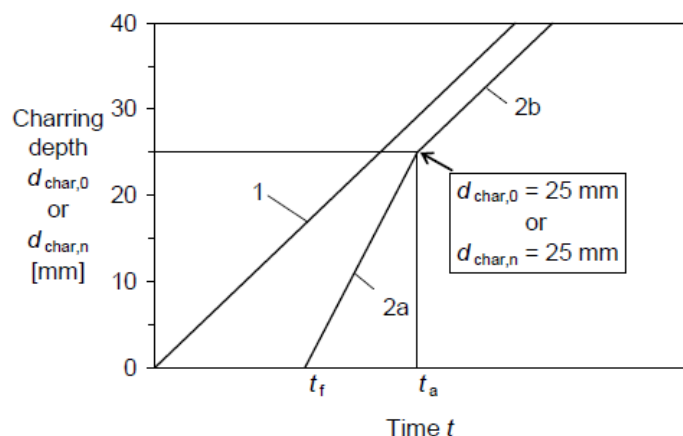


Figure 2.4-1 Charring depth vs time when charring starts at the time of failure [9]

Where t_a is the time when the charring depth reaches 25 mm, t_f is the failure time of the cladding. Line 1 shows the charring rate for unprotected timber members. The initially

protected timber member has a delayed start time of charring (which occurs at the failure time in this example). Charring is more rapid after the failure of the cladding as shown by line 2a. When the char depth reaches 25 mm then the charring rate decreases to the same speed as initially unprotected timber members (line 2b). [9]

Failure time is time from the start of the test when at least 1% of the board has fallen off [10]

If the protection layer stays in place after the start of charring then the charring rate is slowed down significantly compared to charring of an unprotected cross-section (see Figure 2.4-2).

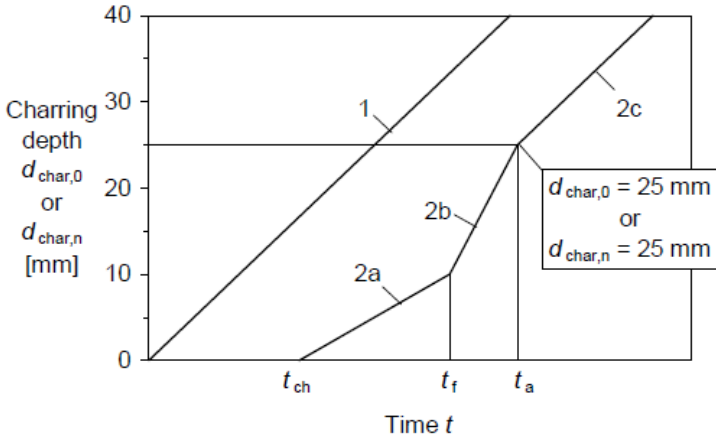


Figure 2.4-2 Charring depth vs time when charring develops behind the cladding [9]

Where t_{ch} is the start time of charring.

Line 1 displays relationship how charring depth changes over time for unprotected timber. Lines 2a, 2b and 2c present the relationship for the protected members where the charring starts before the failure of the cladding. Line 2a shows charring rate in protection phase when the cladding is still intact. Line 2b shows the increased charring rate in the post-protection phase when the cladding has failed. Line 2b shows the charring rate returning to the same speed as initially unprotected members once the charring depth has reached 25 mm. [9]

According to EN 1995-1-2:2004 [9], the start of charring behind gypsum plasterboard type A, H or F is calculated as:

$$t_{ch} = 2.8h_p - 14 \tag{3}$$

Where h_p is the thickness of the panel.

When there are two layers of gypsum plasterboard in cladding then the thickness h_p is the sum of the outer layer and 50% of thickness of the inner layer. When two different types

of gypsum plasterboard are used then the better quality must be the outer layer, while the effectiveness of the inner layers effectiveness is raised to 80%, provided that the spacing of fasteners of the inner layer is not greater than the spacing of fasteners in the outer layer. [9]

For protective claddings made out of wood, gypsum plasterboards type A and H, the failure time t_f should be equal to the start time of charring t_{ch} .

$$t_{ch} = t_f$$

Gypsum plasterboard type F, failure times should be determined by thermal degradation of the cladding or pull-out failure of fasteners due to charring behind the cladding. When type F gypsum board is used then charring starts before failure of the cladding.

$$t_{ch} \leq t_f$$

2.5 Effect of cavity insulation

Most of the joists and studs, in timber frame assemblies, are protected by insulations on lateral sides, however, due to heat flux through the insulation the timber members also char on their lateral sides, resulting in extensive arris roundings. Insulations can be categorised by how well they protect the lateral sides of the timber. [11]

Table 2-2 Protection levels [11]

<p>Protection level 1 (PL1)</p>	<p>Charring develops primarily on the fire-exposed side of the timber, while the lateral sides are semi-protected from the heat and are uncharred. (Figure 2.6-1)</p>
<p>Protection level 2 (PL2)</p>	<p>Charring develops on the fire-exposed side during the protection phase and on all three sides during the post-protection phase due to the reduction of insulation. (Figure 2.6-2)</p>
<p>Protection level 3 (PL3)</p>	<p>Charring develops on all sides during the protection phase. (Figure 2.6-3)</p>

Glass wool, which is mineral wool manufactured from natural sand or molten glass, is considered to be PL2 insulation. The volume of glass wool insulation decreases quickly as the temperature increases. The post-protective behaviour of glass wool insulation is not

comparable with stone wool insulation, although it does provide some small protection after failure of the cladding in comparison with structures with void cavities. [12] [13]

Stone wool, which is mineral wool manufactured from molten naturally occurring igneous rocks, is considered to be PL1 insulation as it is not sensitive to high temperatures. If stone wool batts remain in the cavity after the failure of the cladding then it protects the lateral sides of the beam from the heat. [12]

2.6 Improved design model for timber frame assemblies

The charring scenarios of timber members in timber frame assemblies with cavity insulation are, therefore, dependent on the protection level of the insulation. Additionally, the values of the coefficients are dependent on the insulation. [11]

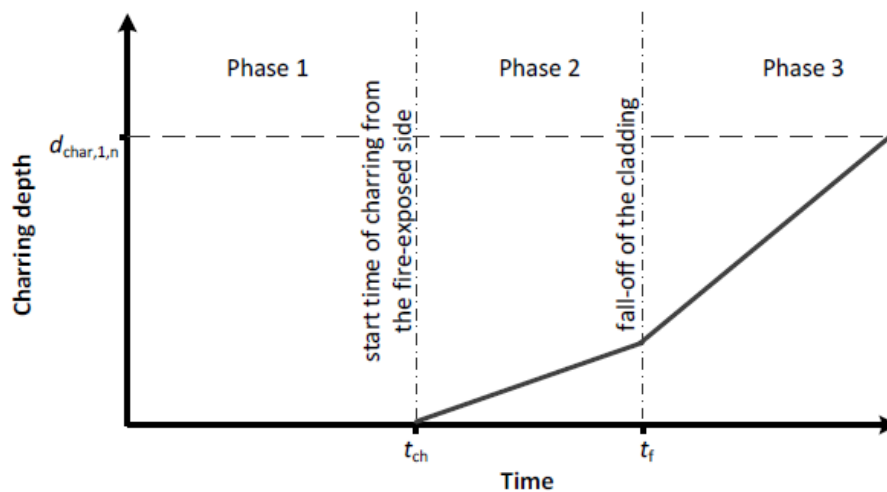


Figure 2.6-1 Protection level 1 [11]

Timber members protected on the lateral sides with PL1 insulation can be considered to char only from the fire exposed side

$$d_{char,1,n} = \beta_0 k_{s,n} k_2 (t_f - t_{ch}) + \beta_0 k_{s,n} k_3 (t - t_f) \quad (4)$$

Where $d_{char,1,n}$ is the notional charring depth, β_0 is the basic charring rate, $k_{s,n}$ is the cross-section factor, k_2 is the protection factor during the protection phase (phase 2), k_3 is the

protection factor in the post-protection phase (phase 3), t_f is the failure time of the cladding, t_{ch} is the start time of charring and t is the total fire exposure time. [11]

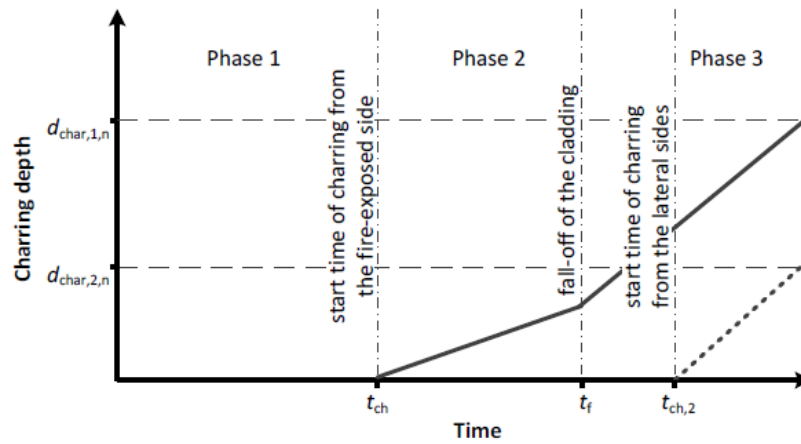


Figure 2.6-2 Protection level 2 [11]

For timber members insulated with PL2 insulation, additional charring on the lateral sides is calculated as:

$$d_{char,2,n} = \beta_0 k_{s,n} k_{3,2} (t - t_{ch,2}) \quad (5)$$

Where $d_{char,2,n}$ is the notional charring depth, β_0 is the basic charring rate, $k_{3,2}$ is the protection factor for the charring on the lateral sides in the post-protection phase, $t_{ch,2}$ is the start time of charring on the lateral sides [8]

$$t_{ch,2} = t_f + \frac{2h}{3v_{rec}} \quad (6)$$

Where, t_f is the failure time of the cladding, h is the height of the beam, v_{rec} is the recession speed for the insulation.

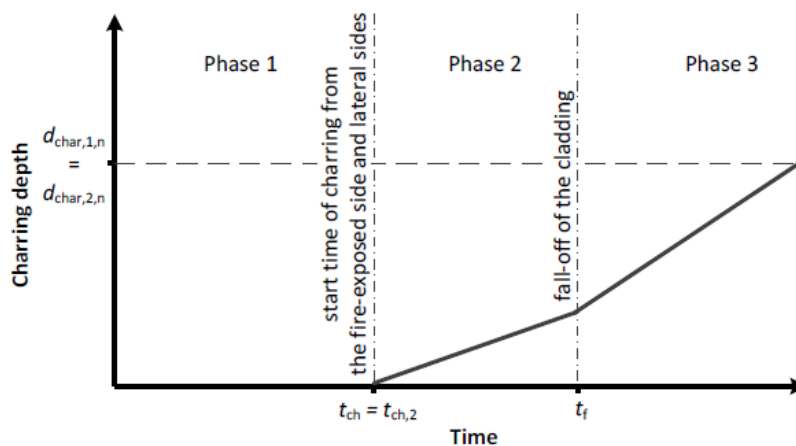


Figure 2.6-3 Protection level 3 [11]

For PL3 insulations, the start of charring on the lateral sides is considered to occur at the same time as the start of charring on the fire exposed side.

According to this categorization PL1 is the best performing. Stone wool (SW) is considered to be a class PL1. Glass wool (GW) products are considered PL2 and expanded polystyrene (EPS) is the worst performing out of the three, falling into category PL3.

The corner rounding factor k_n is equal to 1,5 according to EN 1995-1-2:2004 [9]. This has been proposed by König and Walleij [14]. That the values are between 1.3 and 1.5 and the later is used giving conservative results.

The cross-section factor takes into account that beams with smaller widths char faster. Current EN 1995-1-2:2004 does not give an expression but specifies the values for 38mm, 45mm, and 60mm. The values are derived from the following equation:

$$k_s = \begin{cases} 0,000167b^2 - 0,029b + 2,27 & b \leq 90mm \\ 1 & b > 90mm \end{cases} \quad (7)$$

Where b is the width of the beam [15].

A proposal has been made for design model where cross-section factor $k_{s,n}$ is used. Cross-section coefficient $k_{s,n}$ is derived by multiplying cross-section factor k_s by corner rounding factor k_n . The new factor is independent from the cavity insulation and is expressed as the following equation (9) [11]

$$k_{sn} = \begin{cases} 0,00025b^2 - 0,044b + 3,41 & b \leq 90mm \\ 1,5 & b > 90mm \end{cases} \quad (8)$$

Where b is the width of the beam [8].

When the cladding has fallen off, the post-protection factor k_3 takes into account that the charring rate increases. The charring rate increase is dependent on the cavity insulation used. The expressions are given as a function of failure time of the cladding. [8]

$$k_{3,1} = \begin{cases} 0,022t_f + 1 & t_f \leq 60min \\ 2,32 & t_f > 60min \end{cases} \quad \text{SW} \quad (9)$$

$$k_{3,1} = 0,0171t_f + 1 \quad \text{GW} \quad (10)$$

3 Where t_f is the fall-off time of the cladding. Timber frame assemblies with I-shaped members

3.1 I-joists

Wooden I-joists were invented in 1969 as a substitute for solid lumber. Wood joists are engineered wood assemblies that are optimized to be as efficient as possible in relation to their weight and size. It also shrinks and swells less compared to solid wood. As of 2005, approximately 50% of all wood light framed floors in the USA used I-joists.

The I-joist consists of a web that connects top and lower flanges. The flanges are made of laminated veneer lumber (LVL) or solid wood lumber. The web is most commonly made out of plywood or oriented strand board (OSB). The flanges can be finger jointed, allowing the total length of the beams to be up to 18 meters. One favourable feature of I-joists is that holes can be cut into the webs for the service utilities. Manufacturers provide clear guidelines in their installation guides for the size and location of the holes. [16]

Currently there is no harmonised European standard for I-joists and manufacturer catalogues are the primary source of information. Manufacturers need to apply for an assessment to receive the CE marking. I-joists are available in a wide variety of sizes. Typical I-joists height is from 200mm up to 500mm, flange height is usually from 39 mm to 49mm, and the flange base is from 45 mm to 97mm. Special dimensions could be manufactured by the request of the clients. Leading-I joists manufacturers in Europe are Masonite Beams, STEICO, James Jones and Metsä Wood.

Regardless of who the manufacturer is, the process of making an I-joist is fairly similar. It consists of ripping web material to a specified width. After that the edges and ends of the web are shaped for joining to flanges and adjacent web. Both flanges are grooved to receive the web and are glued with a waterproof glue by pressure fitting the web and the flanges together. Simplified manufacture process can be seen in Figure 3.1-1. [17]

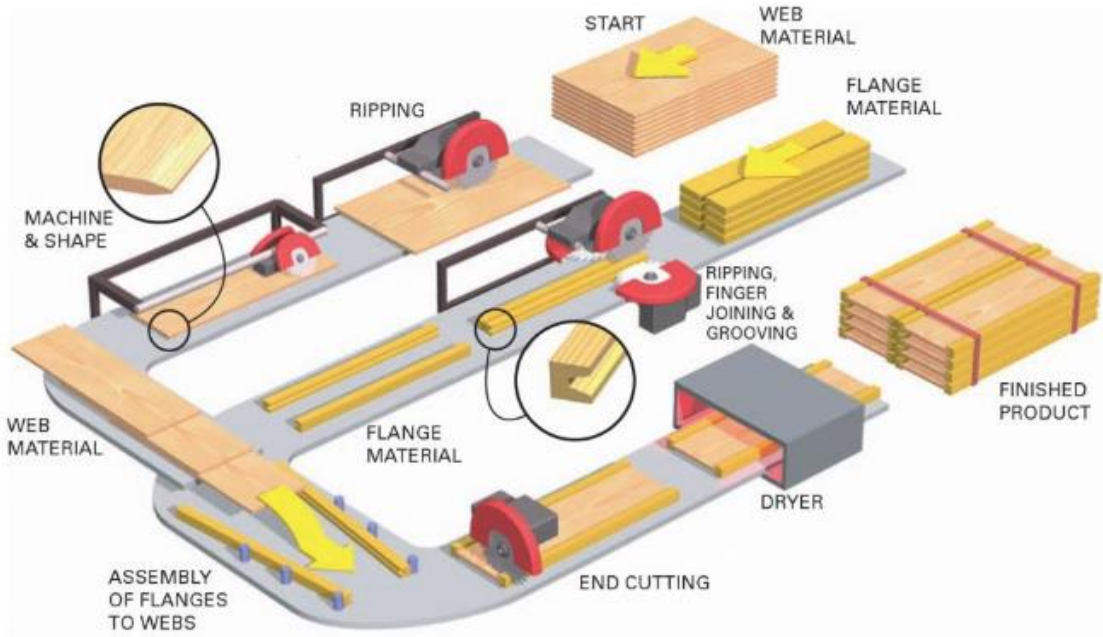


Figure 3.1-1 Manufacture of wood I-joists, simplified

The ability to stack I joists means that significantly less natural resources are required for transportation. The stacking of I-joists is shown in Figure 3.1-2.



Figure 3.1-2 I-joists stacking

3.2 Fire design model

Currently there is no definite fire design model for I-joists. There are two approaches to fire calculations in the European standard. First one is reduced properties method (RPM) where the dimensions of the cross-section are decreased by notional charring depth and strength properties for the residual cross-section are reduced. Second one is an effective cross-section method (ECSM) where the dimensions of the cross-section are decreased by the notional charring depth and zero-strength layer while the strength properties are unaffected. The zero-strength layer compensates for the strength loss of the uncharred wood. The ECSM method is preferred due to its simplicity and will be adopted in the next Fire Safety in Timber buildings is the first technical guideline developed in collaboration with countries across Europe – including Estonia. The guideline is a collection of design codes, European fire standards and classifications. The guideline is easy to comprehend due to many worked examples and case studies. Design model for fire exposed simply supported wooden I-Joists in floor assemblies [18] is included in the published document. [4]

Fire exposed simply supported wooden I-joists in floor assemblies is based on thermal analysis using software SAFIR. From the simulations, a temperature field inside the lower flange of the I-joist was gathered. Charring depth was obtained using 300°C isotherms. The char-line at different time values is given in Figure 3.2-1 [18]

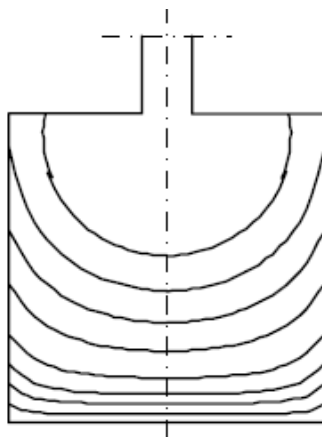


Figure 3.2-1 Propagation of char front in fire-exposed flange [18]

Method described in Fire exposed simply supported wooden I-joists in floor assemblies [18] is limited because an assumption has to be made about failure time of the beam to calculate charring depth.

4 Model scale fire tests

Controlled fire tests need to be carried out in order to evaluate the charring. A model-scale fire test is a representation of a full size fire test. The specimens are smaller, therefore, reducing the cost of building and transportation while still maintaining accurate relationships between all the features of the models. Using model-scale fire tests is a great strategy to investigate the behaviour of materials when exposed to fire. Although the test specimens are quite small, the beams under investigation are not scaled down. The combination of full sized beams with smaller specimen is optimal solution for research. [19]

While testing the fire resistance of a structure, various time-temperature curves can be used. EN 1995-1-2 mostly refers to standard fire exposure (see Figure 3.2-1). The standard temperature-time curve ISO 834 [20] presents a fully developed fire in a compartment. This indicates that it does not account for fire load, ventilation, thermal properties of the enclosure and fire-fighting actions nor the ignition or cooling phase. This allows for direct comparison between many fire tests. [6]

The standard temperature-time curve is expressed by the following equation

$$\theta_g = 20 + 345 \log_{10}(8t + 1) \tag{11}$$

Where θ_g is the gas temperature in the fire compartment, t is the time in minutes.

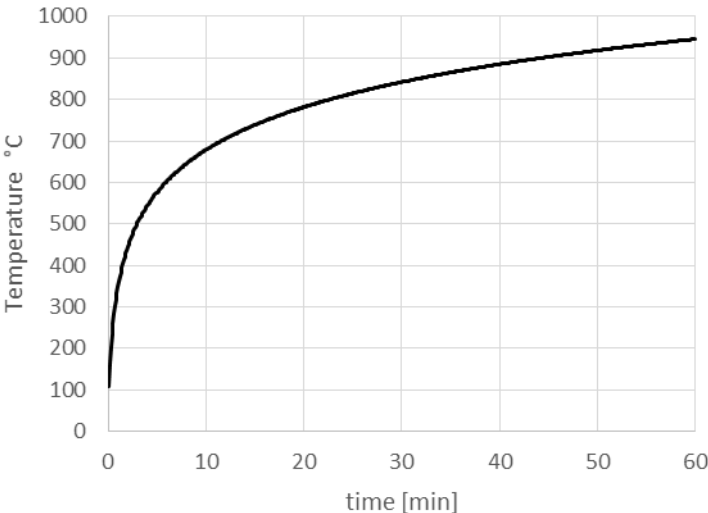


Figure 3.2-1 ISO 834 Standard temperature-time curve [20]

The main purpose of the tests is to generate enough data that can be analysed and to determine the charring depths on the tested beams. A total of 4 tests were conducted – Test 1 (T1) and test 2 (T2) were carried out in Trondheim, Norway on April 29th and 30th 2019. Test 3 (T3) and test (T4) were conducted in Borås, Sweden on December 11th and 13th 2019. (See Table 4-1)

For T1 and T2 a furnace with a volume of 4,5 m³ was used, which had a 1,5m x 1,5m horizontal opening. For T3 and T4 a 1 m³ used that had an opening of 1m x 1m. Both furnaces were equipped with surface plate thermocouples for accurate temperature readings. Both furnaces can to follow ISO 83 temperature-time curve automatically [20].

Table 4-1 Test conducted

Test number	Location	Date
T1	Trondheim, Norway	29.04.2019
T2	Trondheim, Norway	30.04.2019
T3	Borås, Sweden	11.12.2019
T4	Borås, Sweden	13.12.2019

A total of 16 of I-joists were tested between 4 tests. Each beam is numbered according to its test number, cavity insulation and beam type. The marking system is explained in Figure 3.2-2.

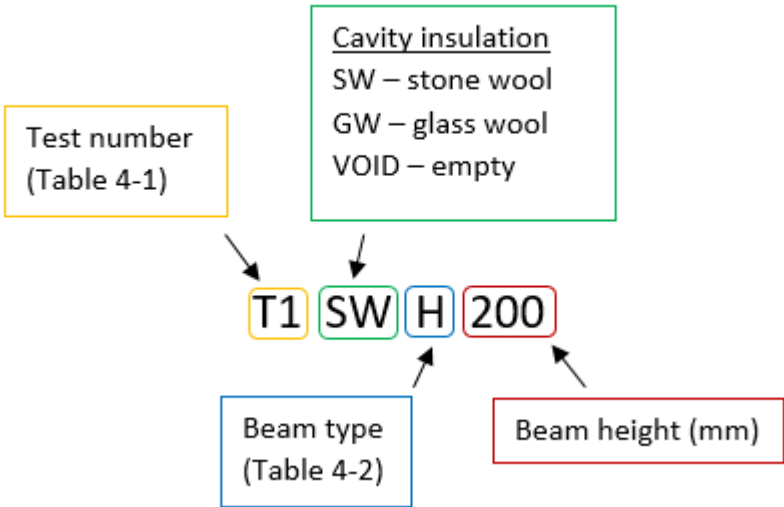


Figure 3.2-2 Marking of tested beams

Beam type is defined by its type of wood and flange dimensions. 4 different types of I-joists were investigated. While beam type H, HI and HB only different by the width of the flange then type LVL has a different flange material. Beam H, HI, HB are mass-produced, while beam LVL was custom made for test 1 and 2. Types of beams tested are presented in Table 4-2

Table 4-2 Tested beam types

Beam	Flange material	Flange height	Flange base
H	Sorted structural timber	47	47
HI	Sorted structural timber	47	70
HB	Sorted structural timber	47	97
LVL	Laminated veneer lumber	39	47

The building of specimens for all the test were generally the same, therefore, the detailed description is given only for April 2019 fire tests.

4.1 April 2019 model scale fire test

4.1.1 Test specimen

The specimens were built at Rundvik in Northern Sweden. Two specimens had the same framework. The outer frame with dimensions 1709 mm by 1709 mm was made out of two I-joists. (See Figure 4.1-1). The cross-section of the specimen is shown in Figure 4.1-2 Cross-section for specimen. The inner member of the framework separated the specimen into two sections. This allowed a total of 6 beams to be tested per specimen – 12 total. A 30 mm fibreboard was used as a web stiffener for the middle framework member. The depth of web stiffener was equal the distance between the flanges of the joists.

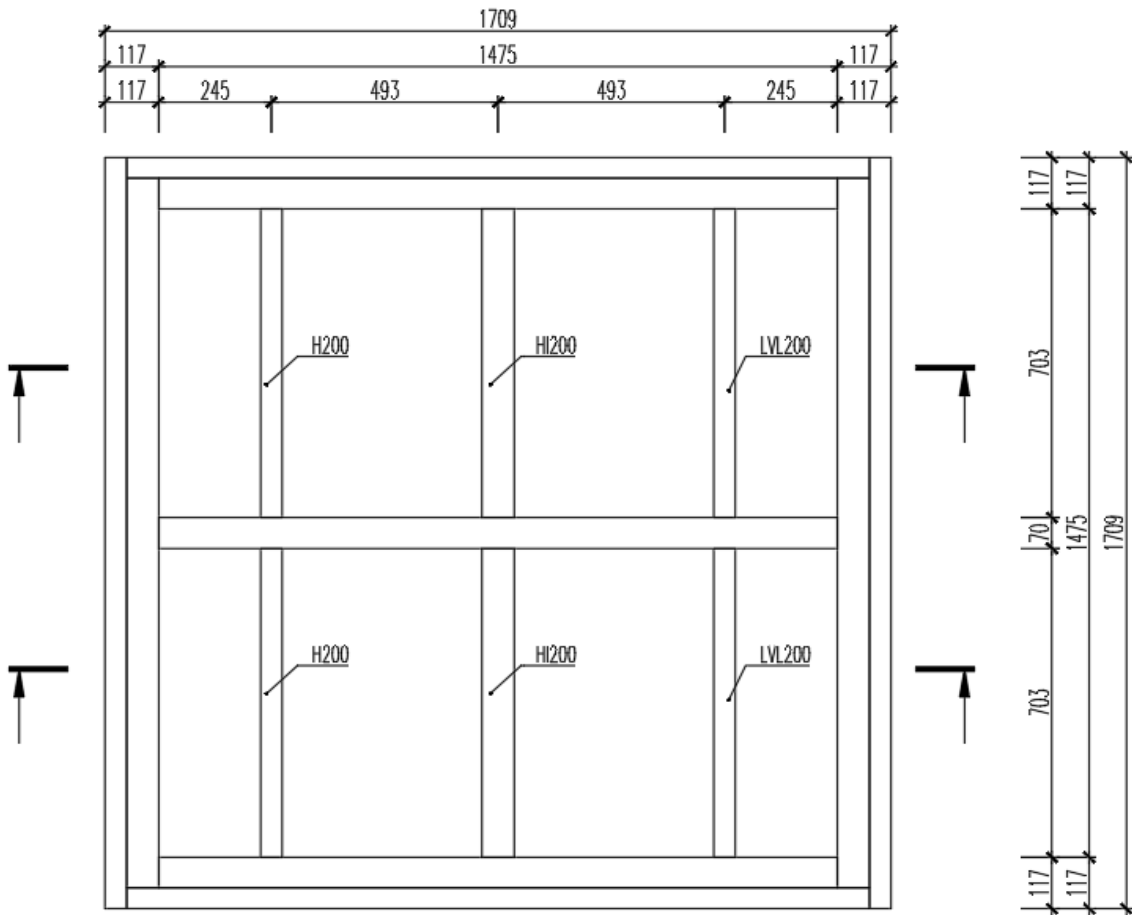


Figure 4.1-1 Framework for T1 and T2

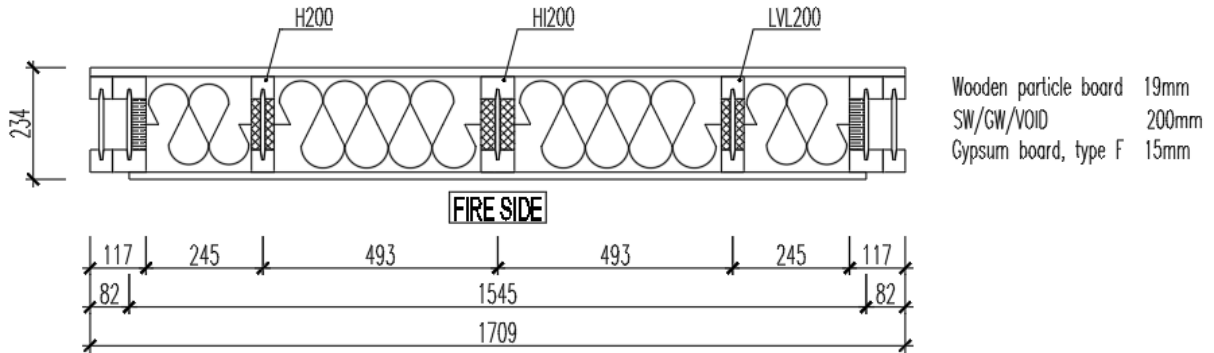


Figure 4.1-2 Cross-section for specimen



Figure 4.1-3 Framework of the specimen

A special I-beam with the lower flange made out of laminated veneer lumber (LVL) was handmade (see Figure 4.1-4), while the two other beams – H200 and HI200 were directly from the production line. The I-beams under investigation were cut to length using mitre saw and a 1.5 mm drill bit was used to make holes for thermocouples inside the lower flange. Every wire was fixed to the appropriate measuring point with staples and tagged with the number. The wires were led out of the specimen between the particleboard and the framework member on the unexposed side (see Figure 4.1-6).

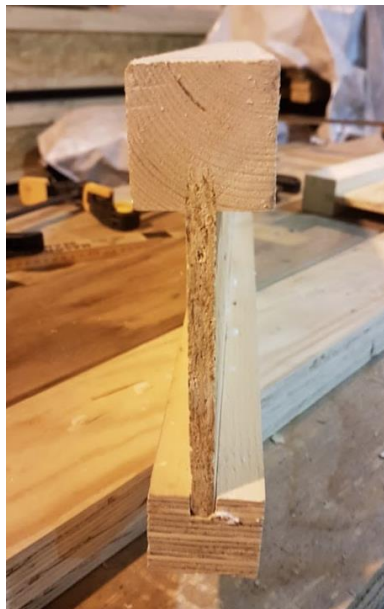


Figure 4.1-4 LVL200 – custom made beam with lower flange made out of laminated veneer lumber.

On the unexposed side a particle board with a thickness of 19 mm was placed for an added stability and to make a closed system. The exposed side was protected by type F gypsum board. A type F gypsum board according to EN 520 [21] is a gypsum board with improved core cohesion at high temperatures. The gypsum boards were installed in two pieces of

770 x 1540 mm. The joint between two gypsum boards was arranged to be on the middle framework beam. A special fastening system was built so board's simulated falling off could be imposed. The system composed on a screw thread metal bar. On the fire-exposed side a combination of two washers and a hex nut held the gypsum board in place for a fixed period of time. On the unexposed side a hole was drilled through the metal bar and a single coil retraining clip (R-clip) was placed through it which was the only element of the system holding the gypsum board in place. Therefore, by removing the R-clips the gypsum boards would fall into the furnace. (see Figure 4.1-5)

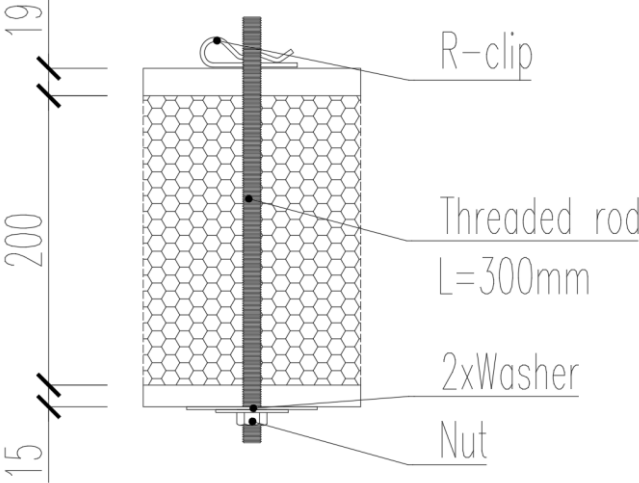


Figure 4.1-5 R-clip system for supporting the gypsum board



Figure 4.1-6 Construction of the specimen – thermocouples installed, screwing in the wooden particle board

Webbing insulations and cavity insulations were cut into size. Glass and stone wool were over dimensioned from all side 5 mm to assure that they do not fall out when the cladding is removed. Furthermore, a caulking gun was used to spread a silicate glue

evenly onto the particle board and onto the web. Insulations were installed and slightly pressed to ensure that the glue makes contact with the insulation.



Figure 4.1-7 Construction of the specimen – installing the insulation

Due to the size of the specimen, the gypsum plasterboard cladding was installed in two pieces. The dimensions of one piece was 1540 x 770 mm. The joint between the plasterboards was aligned with the middle framework beam. To ensure that the gypsum board does not move during the transport and during the installation of the metal fastening system, four screws were screwed into the each corner of the plasterboard.



Figure 4.1-8 Construction of the specimen-installing the plasterboard

Table 4-3 Thicknesses of the components

Component	Thickness mm
Gypsum plasterboard, type F	15
I joists / Insulation	200
Wooden particle board	19

Various types of insulation were used as webbing insulation and as cavity insulations. Different combinations are presented in Table 4-4.

Table 4-4 Tested beams; expanded polystyrene (EPS), Stone wool (SW), glass wool (GW)

Test	Marker	Dimensions of the flange (BxH) (mm)	Web Insulation	Cavity insulation
Test 1	T1 SW H200	47x47	EPS	SW
	T1 SW HI200	70x47	EPS	SW
	T1 SW LVL200	47x39	EPS	SW
	T1 SW H200	47x47	SW	SW
	T1 SW HI200	70x47	SW	SW
	T1 SW LVL200	47x39	SW	SW
Test 2	T2 VOID H200	47x47	EPS	VOID
	T2 VOID HI200	70x47	EPS	VOID
	T2 VOID LVL200	47x39	EPS	VOID
	T2 GW H200	47x47	GW	GW
	T2 GW HI200	70x47	GW	GW
	T2 GW LVL200	47x39	GW	GW

Thermocouples for I-beams under investigation were placed in the midpoint of the span. Also, multiple thermocouples were placed between the insulation and the particleboard. Thermocouples behind the insulation are able to signal when the particle board starts charring (Figure 4.1-9). Thermocouples were fixed in position with a stapler.

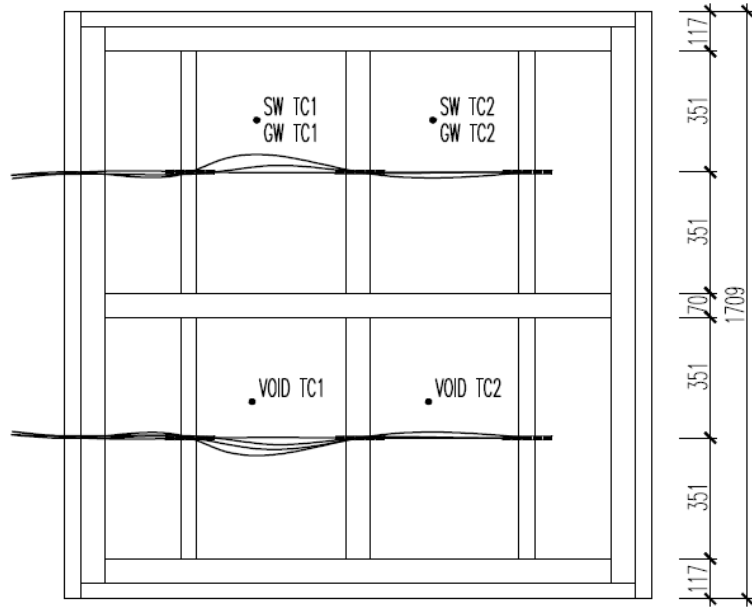


Figure 4.1-9 Thermocouple placements

All the thermocouples were type K with an external diameter of 1mm. Figure 4.1-10 shows exact location of the thermocouples placed. The holes for the wires were drilled from the side of the member in a zig-zag pattern (Figure 4.1-11). Thermocouple wires were crimped (twisted length 3mm).

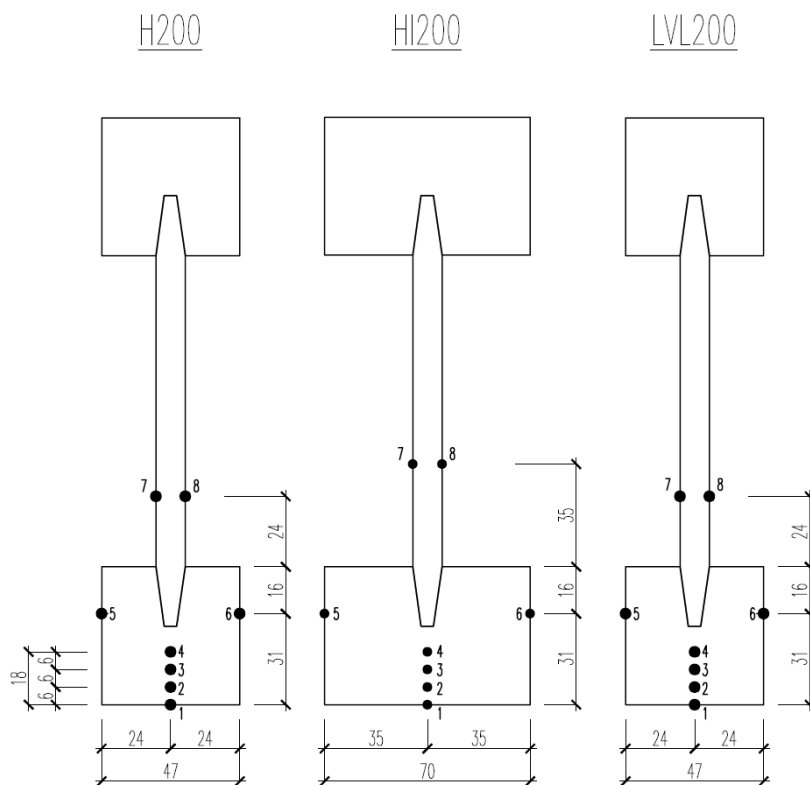


Figure 4.1-10 Location of the thermocouples – cross-section

Figure 4.1-11 and Figure 4.1-12 illustrate where holes for thermocouples were drilled, each hole is offset 5mm from the next one. This assures that every thermocouple is surrounded by solid wood that has not been damaged. This ensures that thermocouple temperature readings are not affected by the previously drilled holes.

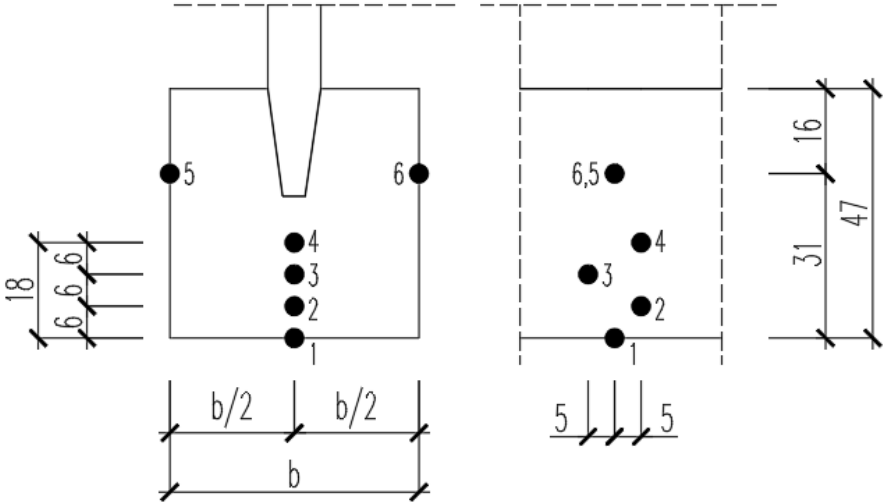


Figure 4.1-11 Location of the thermocouples – cross-section and side view



Figure 4.1-12 Location of the thermocouples – side view

4.1.2 Test description

Test specimens were transported from Rundvik to a laboratory in Trondheim. A furnace with a volume of 4,5m³ was used for both tests. Before the fire test, type K male connectors were installed and a layer of calcium silicate insulation was placed around the edge of the furnace to make it airtight. Specimens were lifted on top of a furnace with the help of an overhead crane and placed in a horizontal position. Pre-test procedures were identical for both of the specimens (Figure 4.1-13).

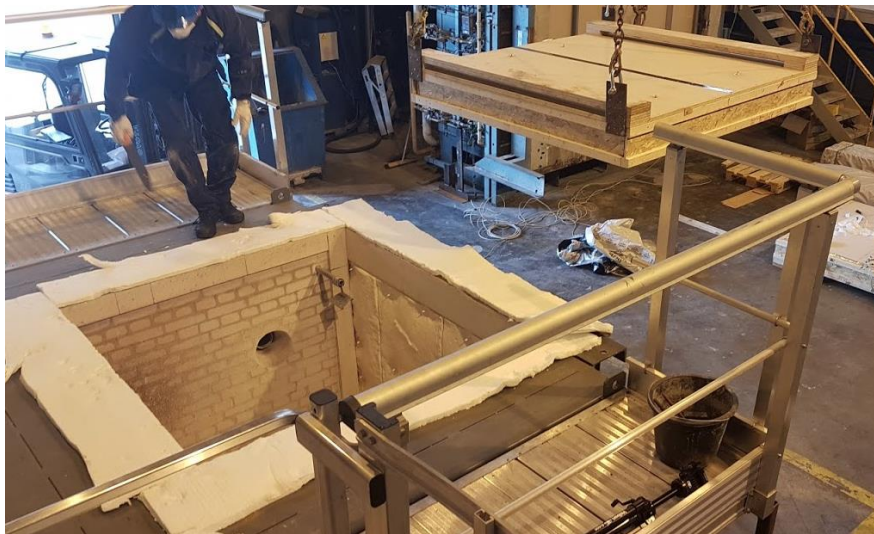


Figure 4.1-13 Installing the specimen on top of the furnace

After the installation of the specimen on top of the furnace, all the thermocouples were connected to a measurement device and their ID numbers noted (Figure 4.1-14).



Figure 4.1-14 Thermocouple connectors

The duration of test 1 (T1) was 43 minutes and test 2 (T2) was 37 minutes (Table 4-5). During T1 5 minutes into the test, some smoke was seen coming out from the corner of the specimen. The problem was solved for the second test by filling the empty caps in the corner full of the same insulation that was placed on the edge of the furnace.

Table 4-5 Duration of the tests 1 and 2

Test	Duration (min)
T1	43
T2	37

After the fire tests were terminated, the specimens removed from the furnace and extinguished within 5 minutes.



Figure 4.1-15 Extinguishment

After the specimens cooled completely a section from each I beam was cut out using a handheld saw and marked with an ID. Residual cross-sections are presented in heading 5.4.

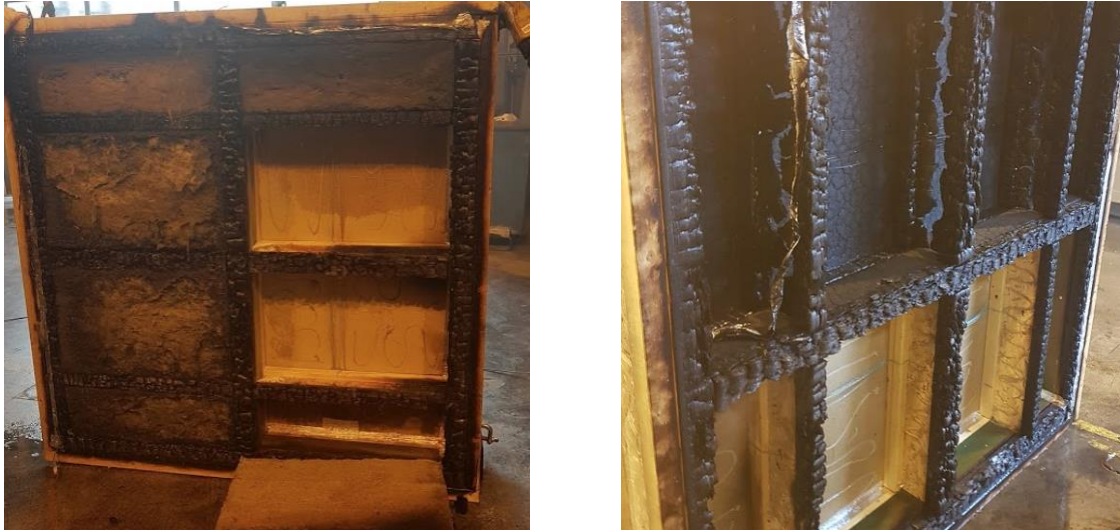


Figure 4.1-16 Specimens after the test; T1 on the left and T2 on the right

Char was removed from the cross-section using a steel brush. Everything that stays on the cross-section after a thorough cleaning with a brush is considered to be wood.

4.1.3 Test results

The fire exposure was started and the temperature in the furnace was increased following the standard fire temperature-time curve according to ISO 834 [20]. Recorded data for furnace temperature and can be found in Figure 4.1-17 and pressure in Figure 4.1-18.

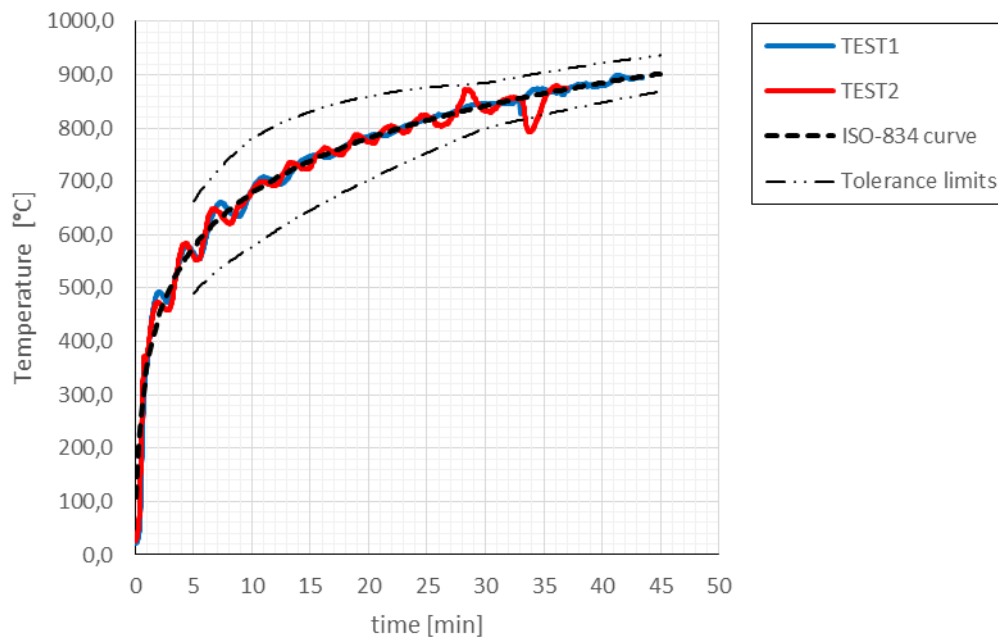


Figure 4.1-17 Furnace Temperature

Although no tolerances are given for the first 5 minutes of the fire test, laboratory attempted to follow the temperature-time curve as closely as possible. The sudden drop in temperature at 34 minutes for test 2 is due to the failure of the gypsum board that suffocated the fire. Deviation lasted for 2 minutes and is not considered detrimental for test results.

Table 4-6 Furnace temperature tolerances [22]

Deviation limit [%]	Time [min]
15	$5 < t \leq 10$
$(15 - 0,5(t - 10))$	$10 < t \leq 30$
$(5 - 0,083(t - 30))$	$30 < t \leq 60$

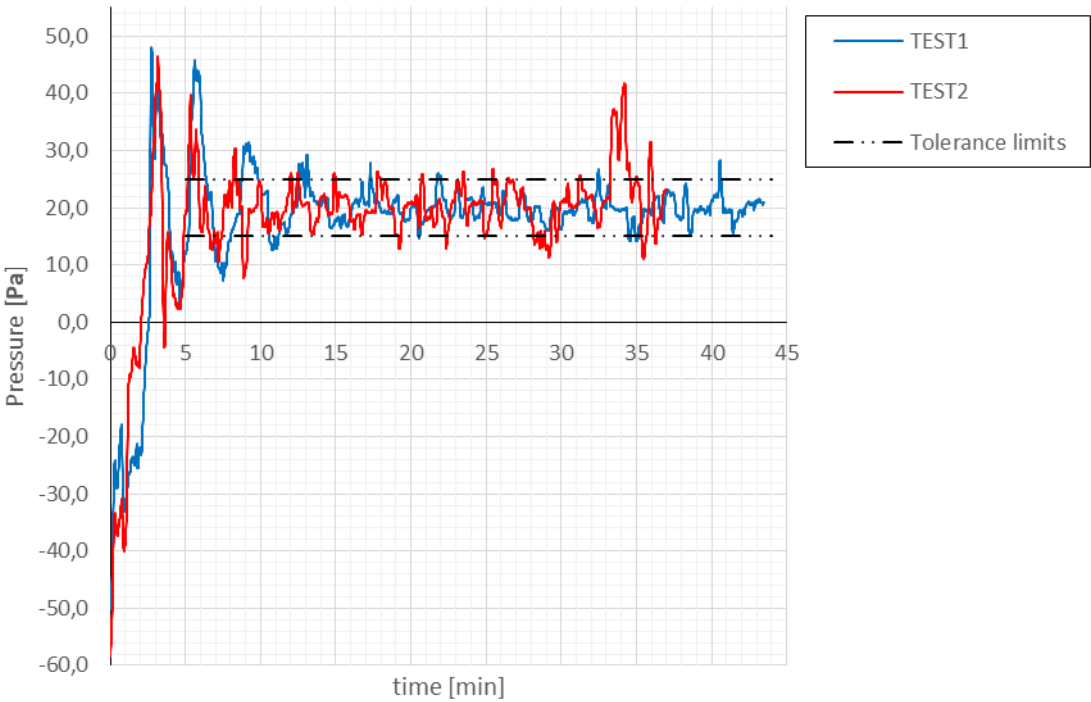


Figure 4.1-18. Furnace pressure

Positive air pressure is a requirement for fire tests. That means air pressure inside the furnace is greater than the pressure outside and smoke will attempt to escape through the specimen. These tests were done to investigate the charring of the I-beams, not integrity of the structure and therefore air pressure is not a critical parameter.

Thermocouples recorded temperatures every 1.2 seconds. These temperature changes are shown on a time-temperature graph for each thermocouple position on Figure 4.1-19 to Figure 4.1-30. When the thermocouple records 300°C then charring has reached that particular point.

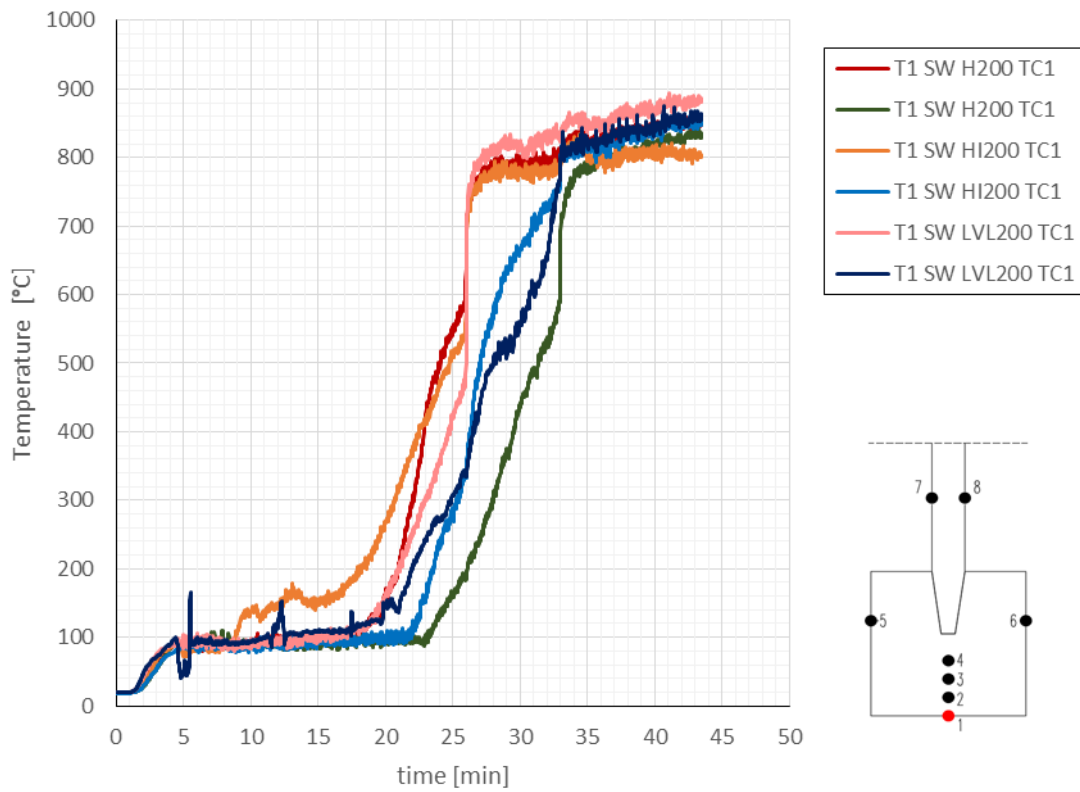


Figure 4.1-19 Thermocouple 1 (TC1) readings for I-beams tested in test 1 (T1)

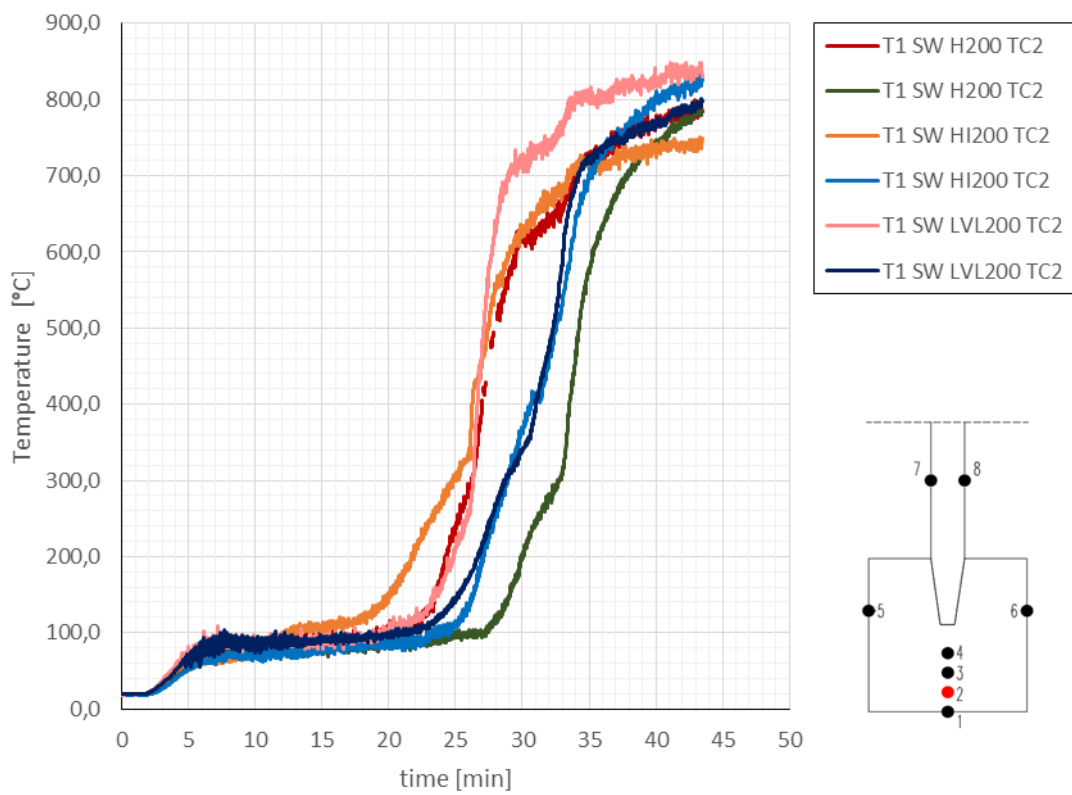


Figure 4.1-20 Thermocouple 2 (TC2) readings for I-beams tested in test 1 (T1)

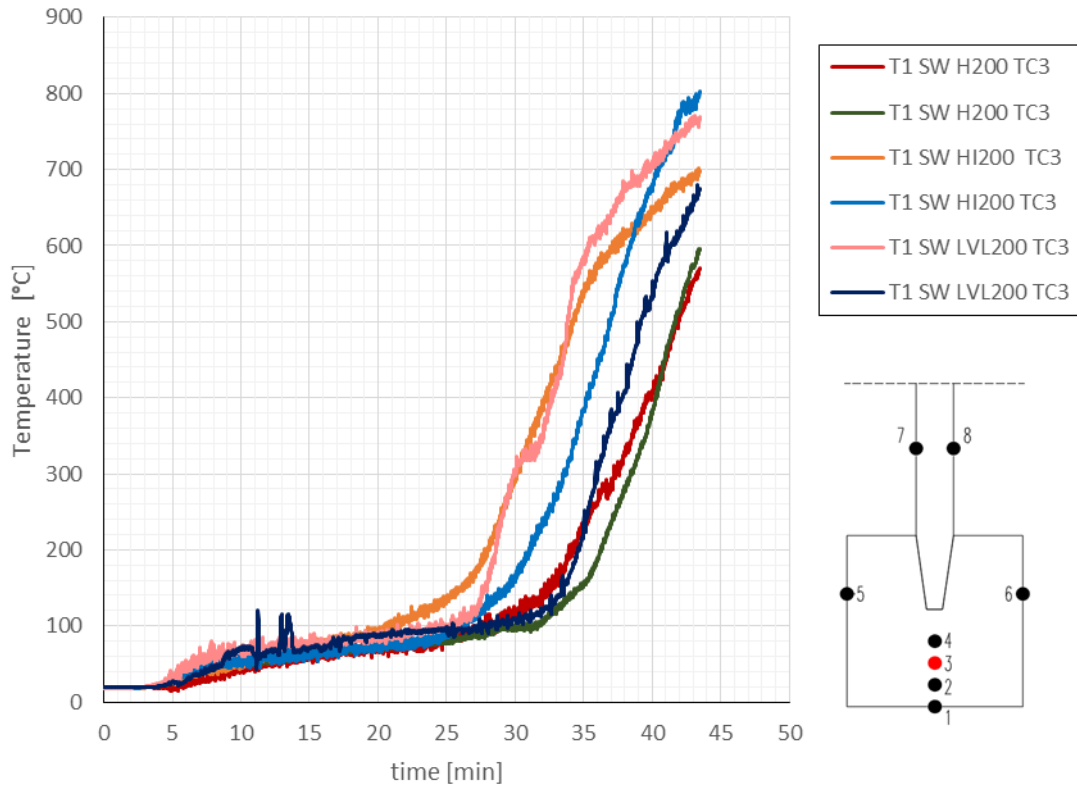


Figure 4.1-21 Thermocouple 3 (TC3) readings for I-beams tested in test 1 (T1)

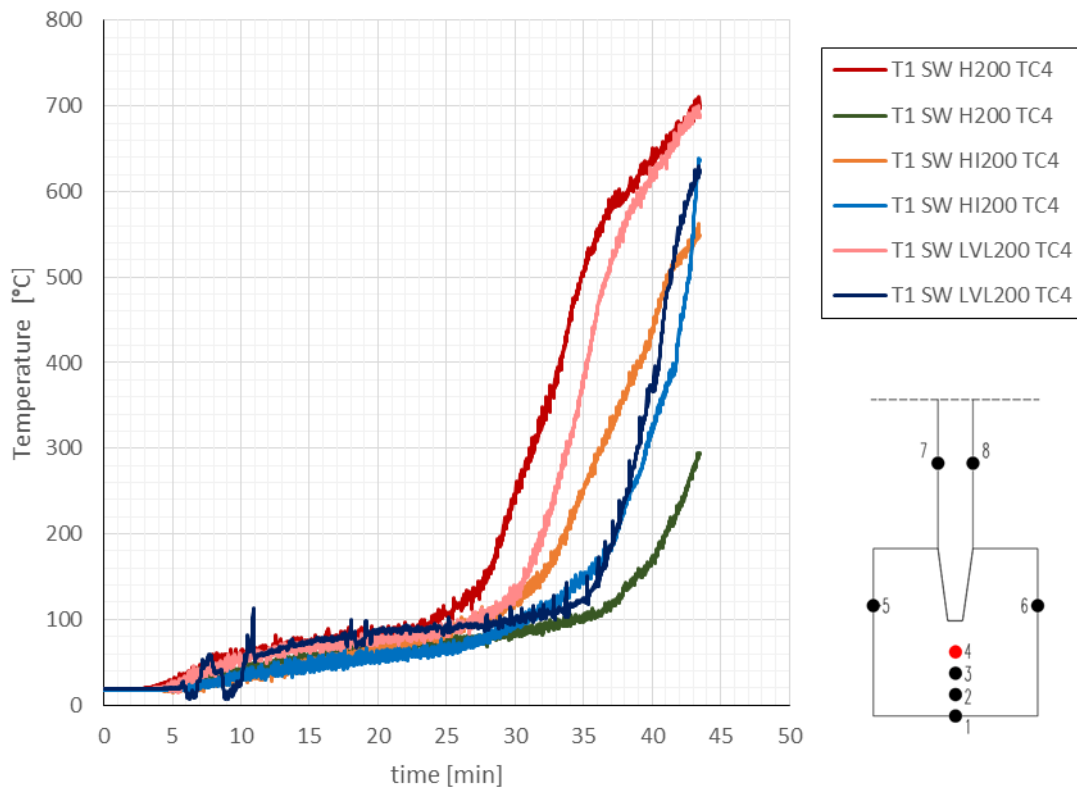


Figure 4.1-22 Thermocouple 4 (TC4) readings for I-beams tested in test 1 (T1)

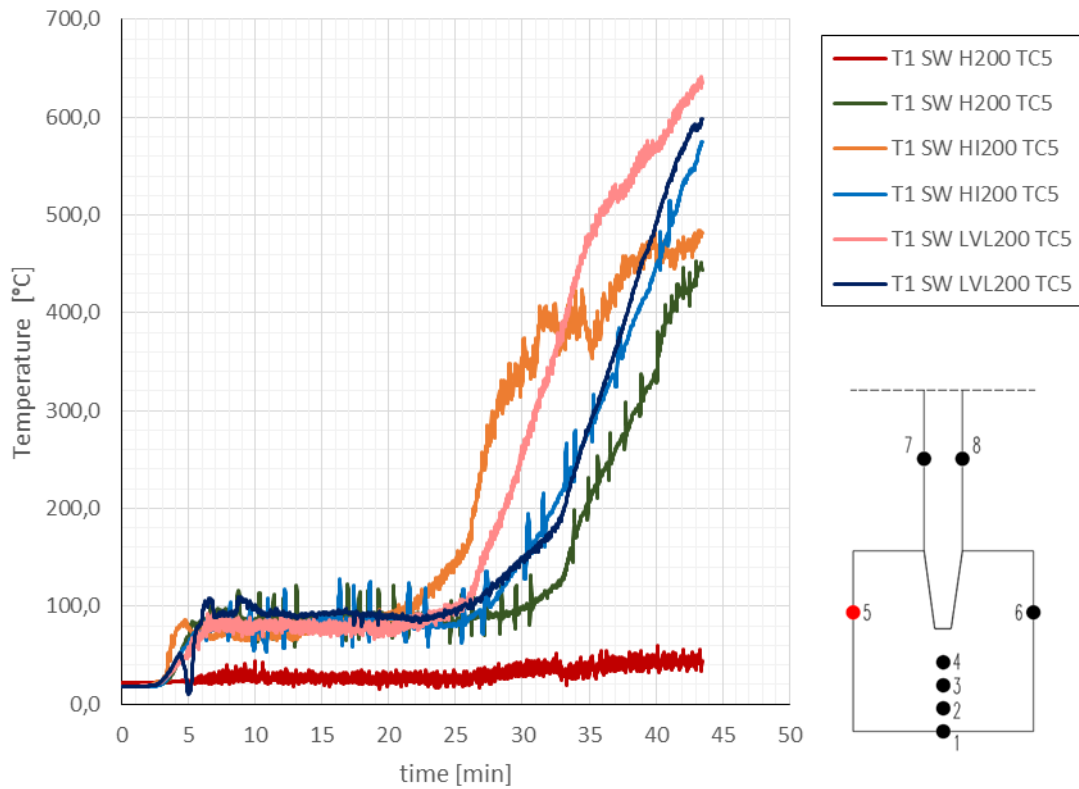


Figure 4.1-23 Thermocouple 5 (TC5) readings for I-beams tested in test 1 (T1)

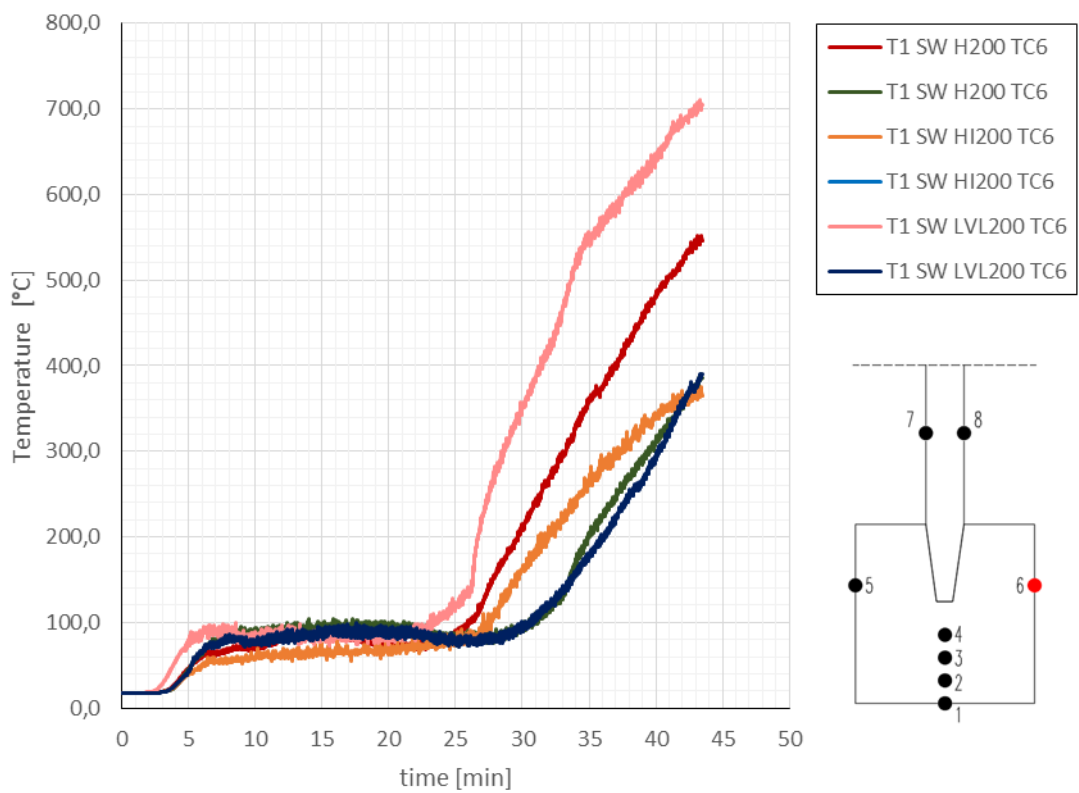


Figure 4.1-24 Thermocouple 6 (TC6) readings for I-beams tested in test 1 (T1)

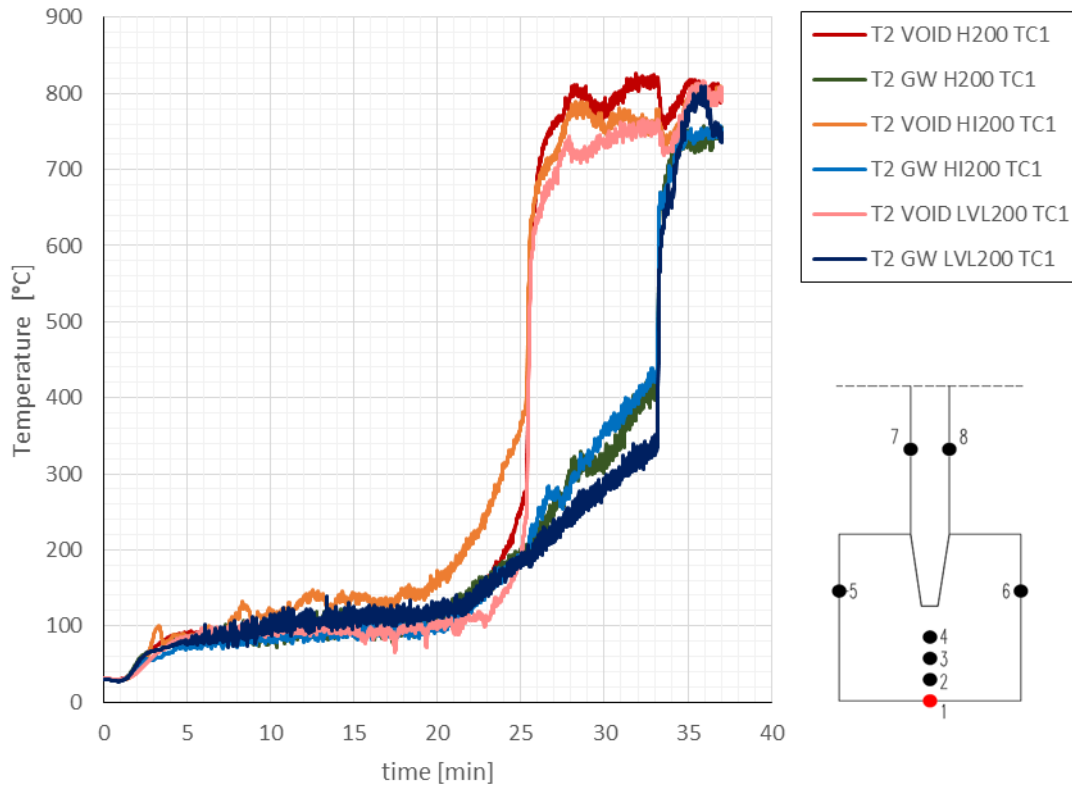


Figure 4.1-25 Thermocouple 1 (TC1) readings for I-beams tested in test 2 (T2)

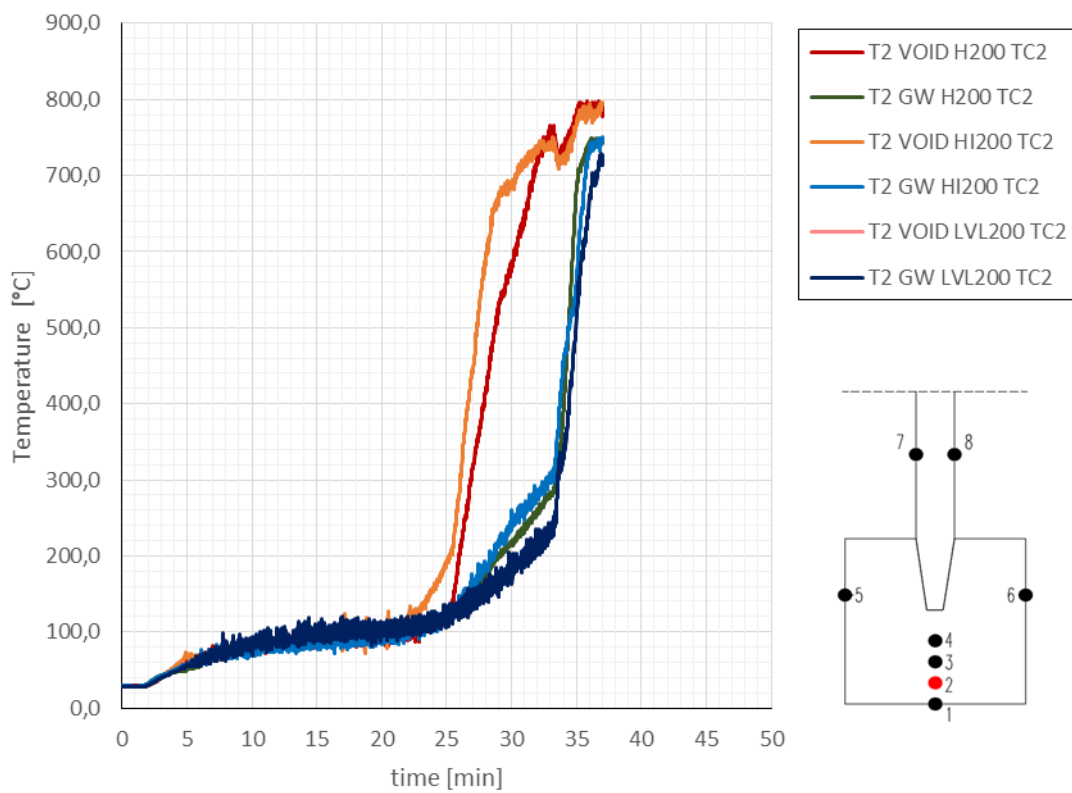


Figure 4.1-26 Thermocouple 2 (TC2) readings for I-beams tested in test 2 (T2)

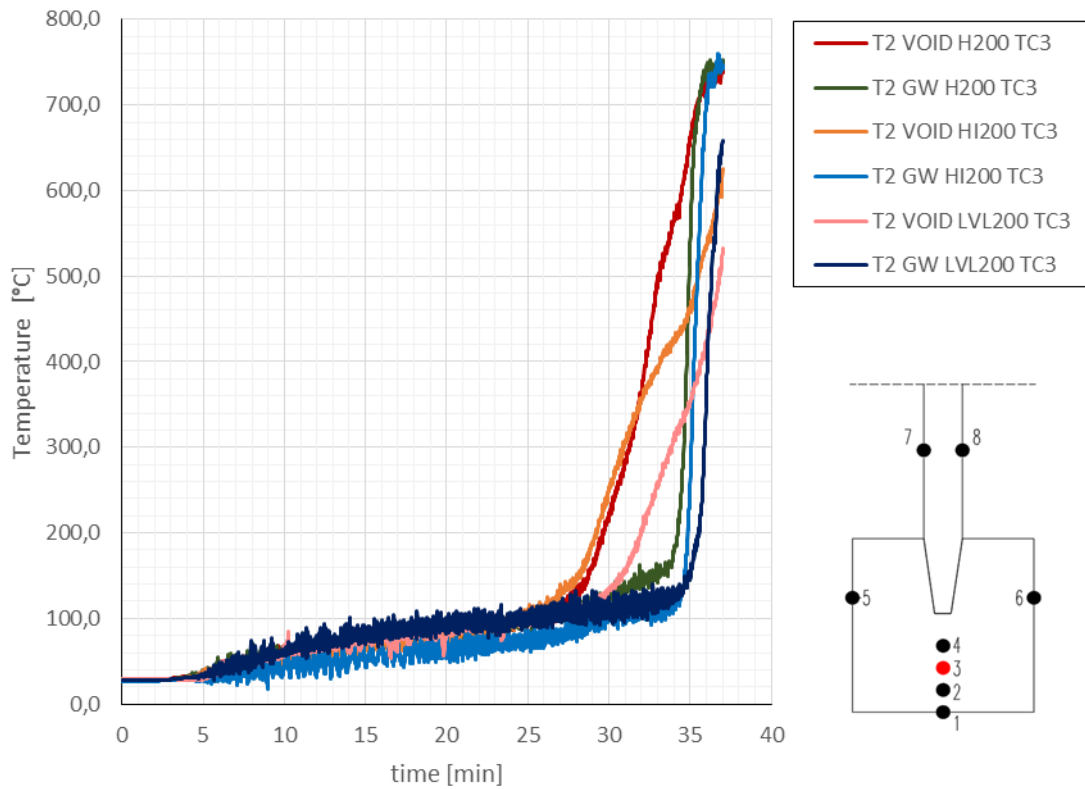


Figure 4.1-27 Thermocouple 3 (TC3) readings for I-beams tested in test 2 (T2)

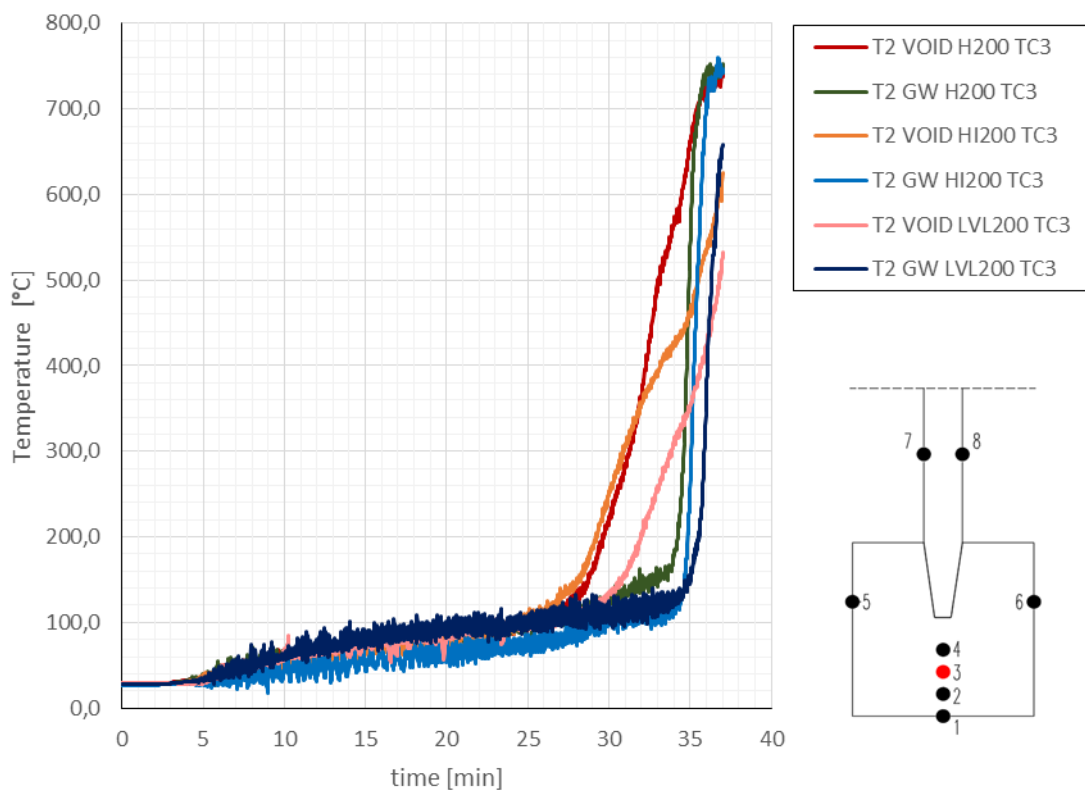


Figure 4.1-28 Thermocouple 4 (TC4) readings for I-beams tested in test 2 (T2)

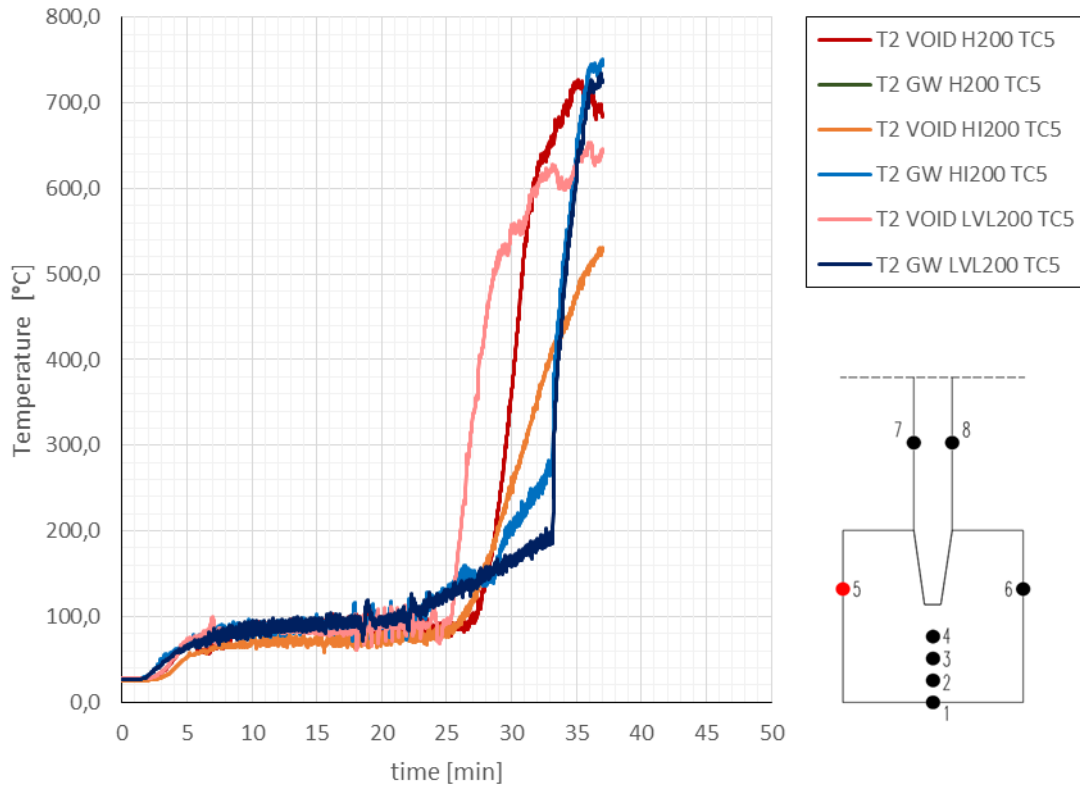


Figure 4.1-29 Thermocouple 5 (TC5) readings for I-beams tested in test 2 (T2)

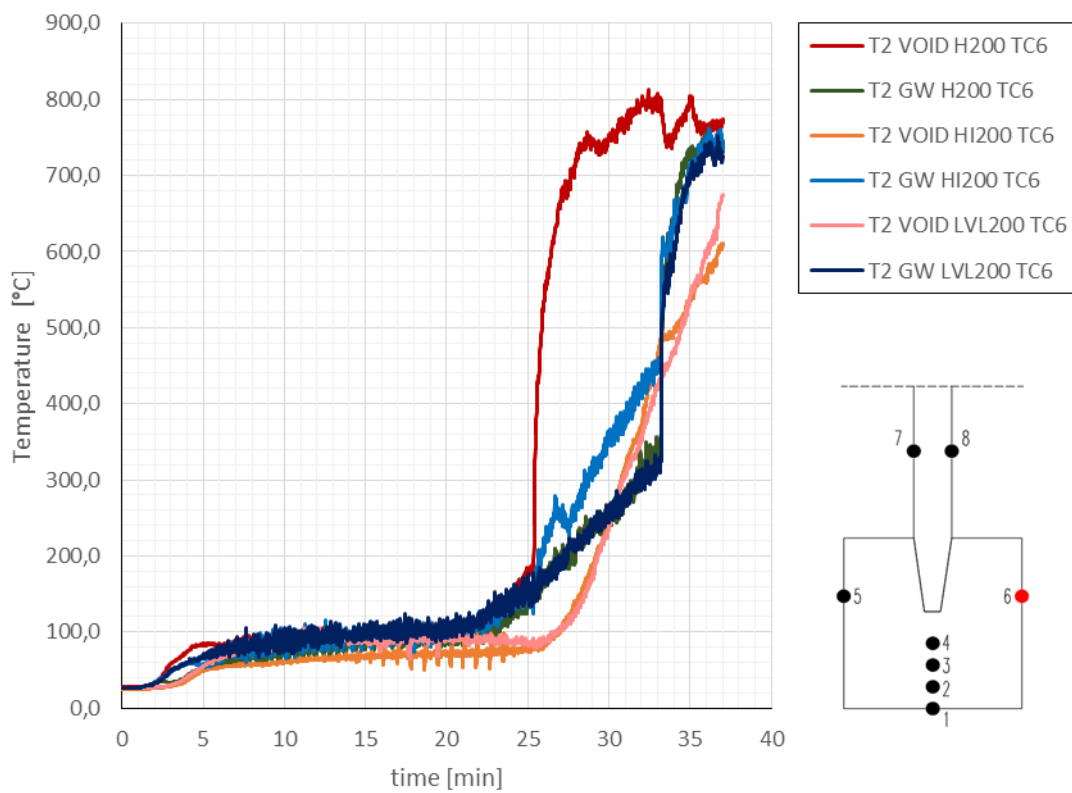


Figure 4.1-30 Thermocouple 6 (TC6) readings for I-beams tested in test 2 (T2)

4.2 December 2019 model scale fire test

4.2.1 Test specimen

Additional two specimen were built with outer dimensions of 1098 x 1098mm (Figure 4.2-1). This allowed for two I-joist to be investigated per specimen – 4 total. Both specimen were identical besides the different cavity insulation.

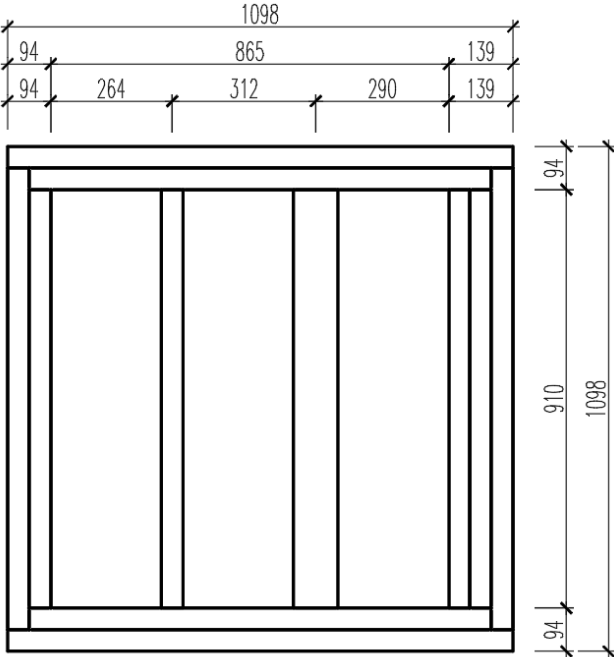


Figure 4.2-1 Framework for T3 and T4

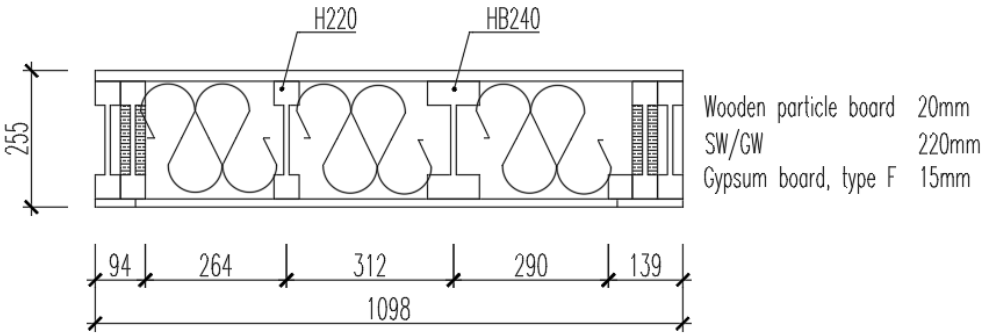


Figure 4.2-2 Cross-section for T3 and T4, fire from the bottom

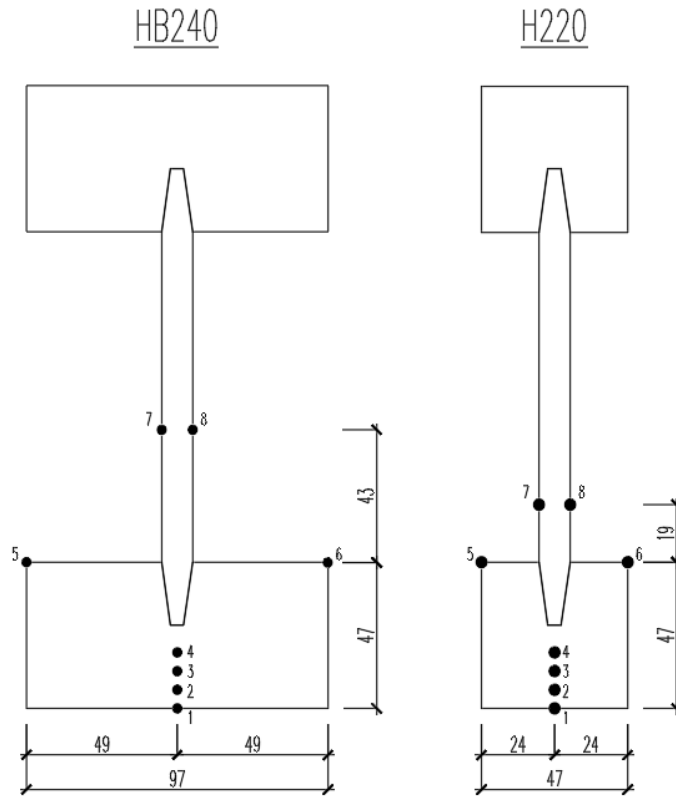


Figure 4.2-3 Thermocouple placements for T3 and T4

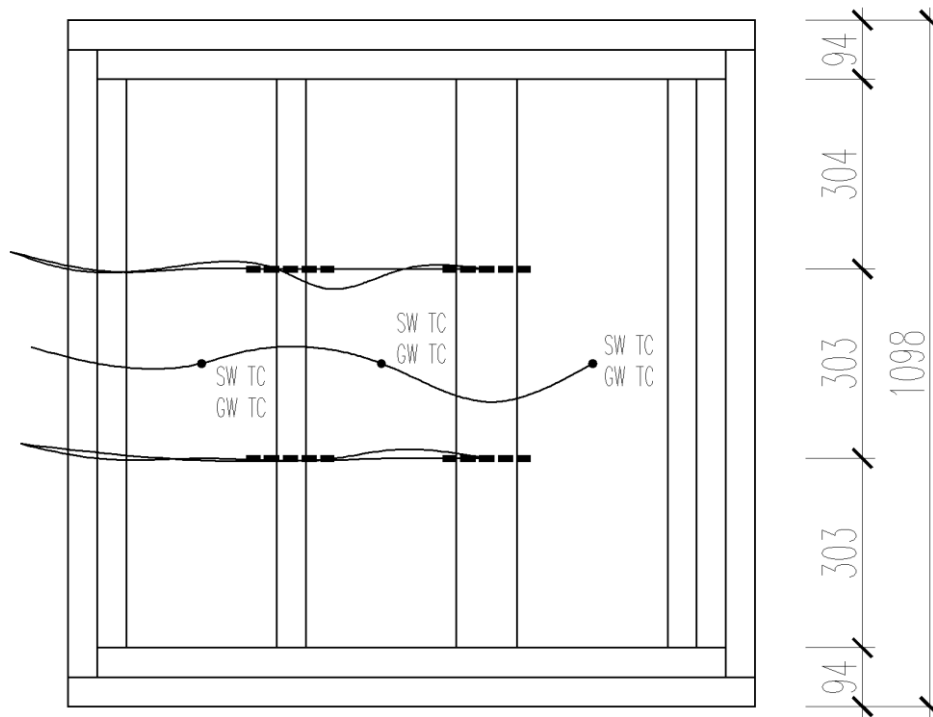


Figure 4.2-4 Thermocouple locations for T3 and T4

Three thermocouples were placed in the cavities, between the gypsum board and insulation. These thermocouples were installed to register fall-off time of the cladding.

Table 4-7 Tested beams

Test	Marker	Web Insulation	Cavity insulation
Test 3	T3 GW H220	GW	GW
	T3 GW H220	GW	GW
	T3 GW HB240	GW	GW
	T3 GW HB240	GW	GW
Test 4	T4 SW H220	SW	SW
	T4 SW H220	SW	SW
	T4 SW HB240	SW	SW
	T4 SW HB240	SW	SW

4.2.2 Test description

The duration of test 3 (T3) was 46,4 minutes and test 4 (T4) was 70,1 minutes.

Table 4-8 Duration of the tests 3 and 4

Test	Duration (min)
T3	46,4
T4	70,1

After the fire tests were terminated, the specimens removed from the furnace and extinguished within 5 minutes.

4.2.3 Test results

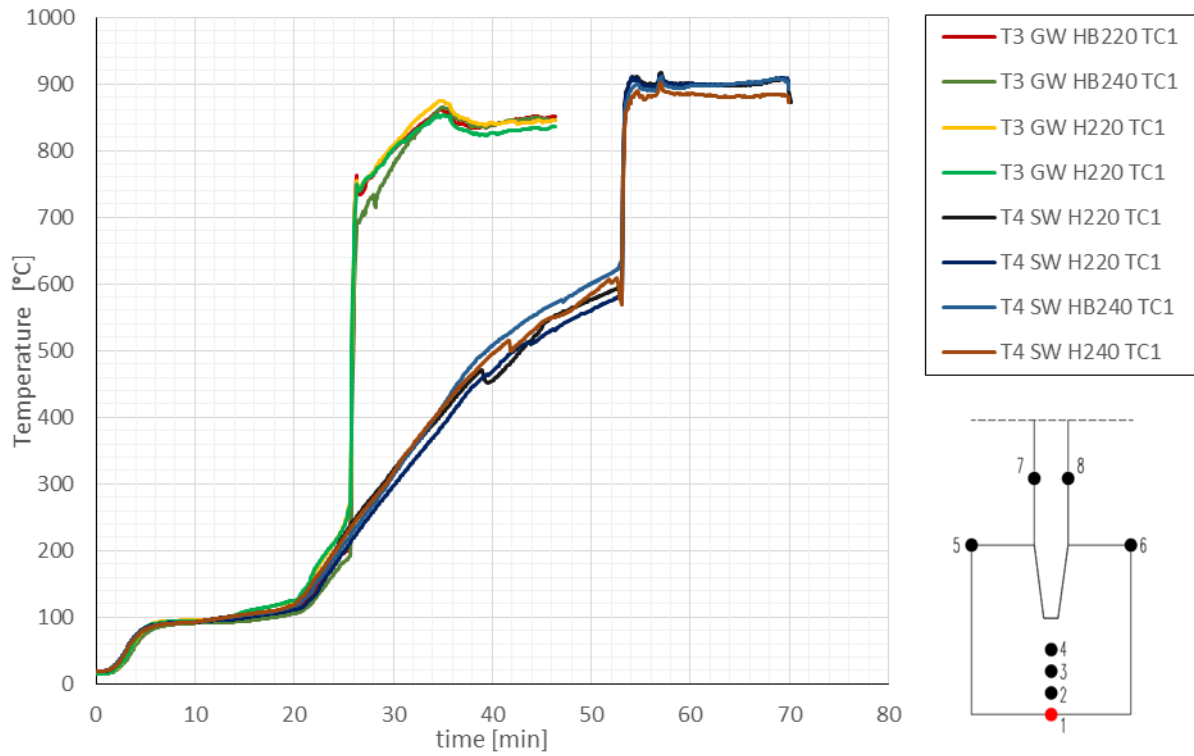


Figure 4.2-5 Thermocouple 1 (TC1) reading for I-beams tested in T3; T4

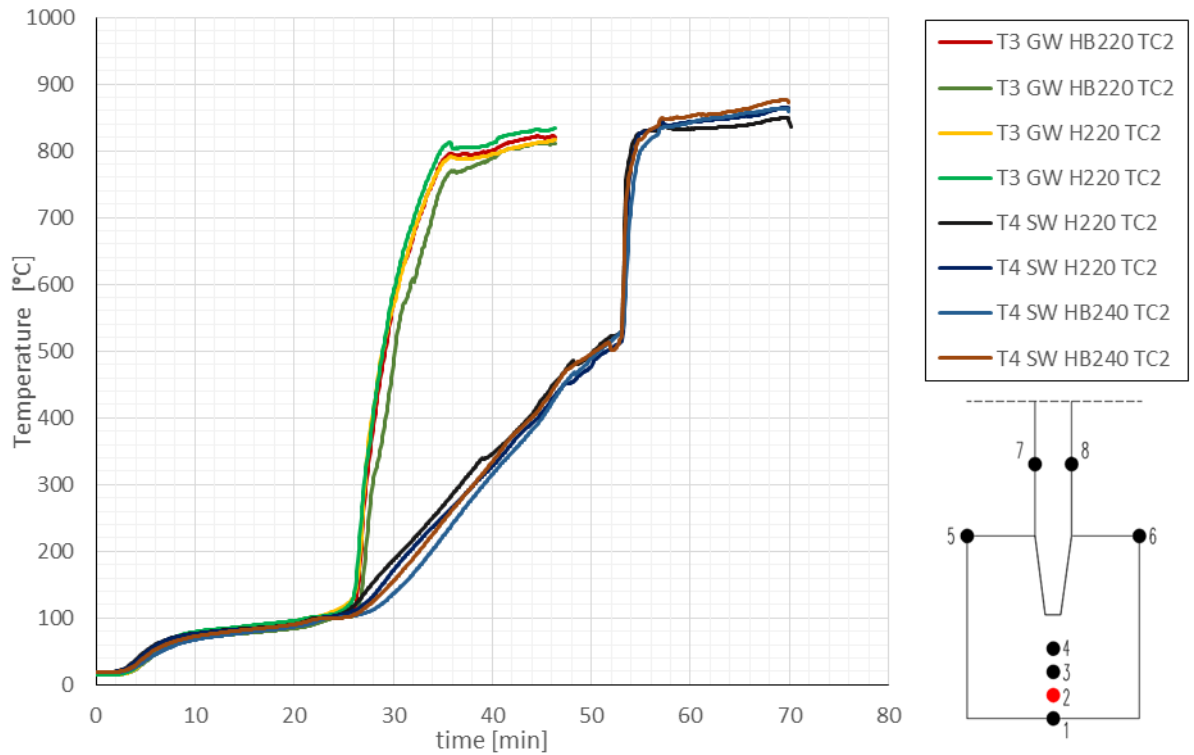


Figure 4.2-6 Thermocouple 2 (TC2) reading for I-beams tested in T3; T4

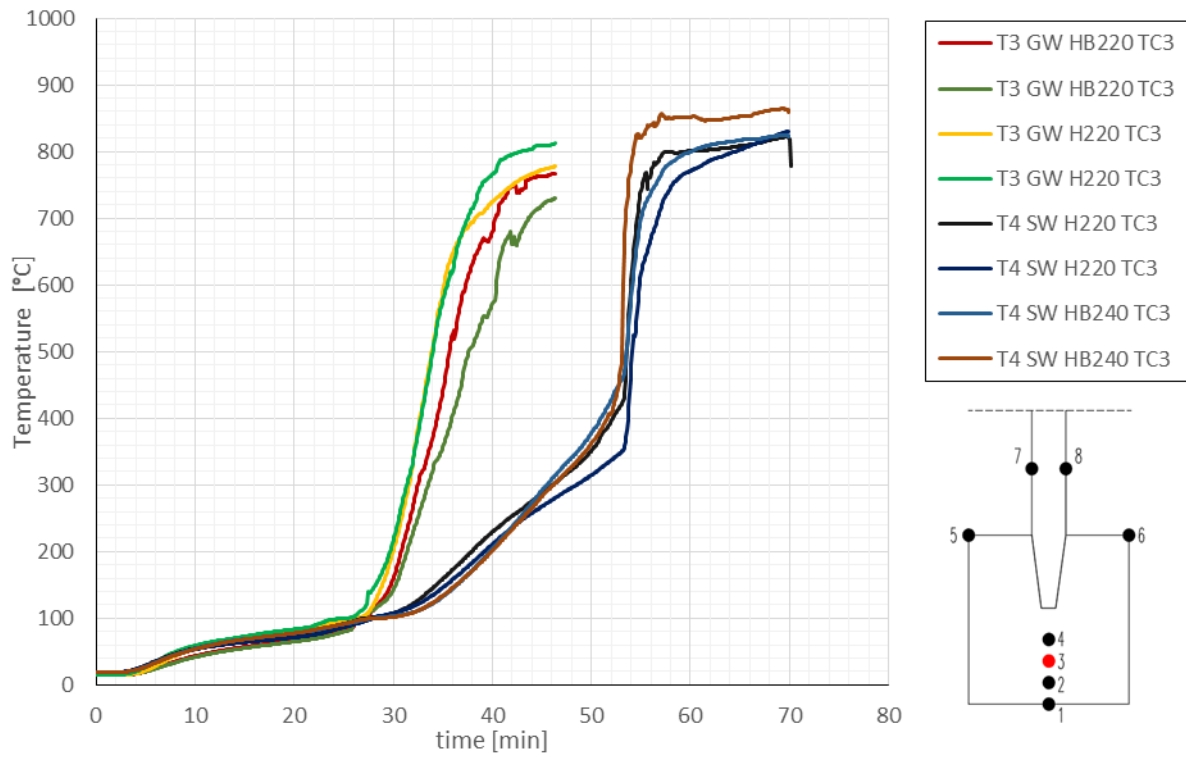


Figure 4.2-7 Thermocouple 3 (TC3) reading for I-beams tested in T3; T4

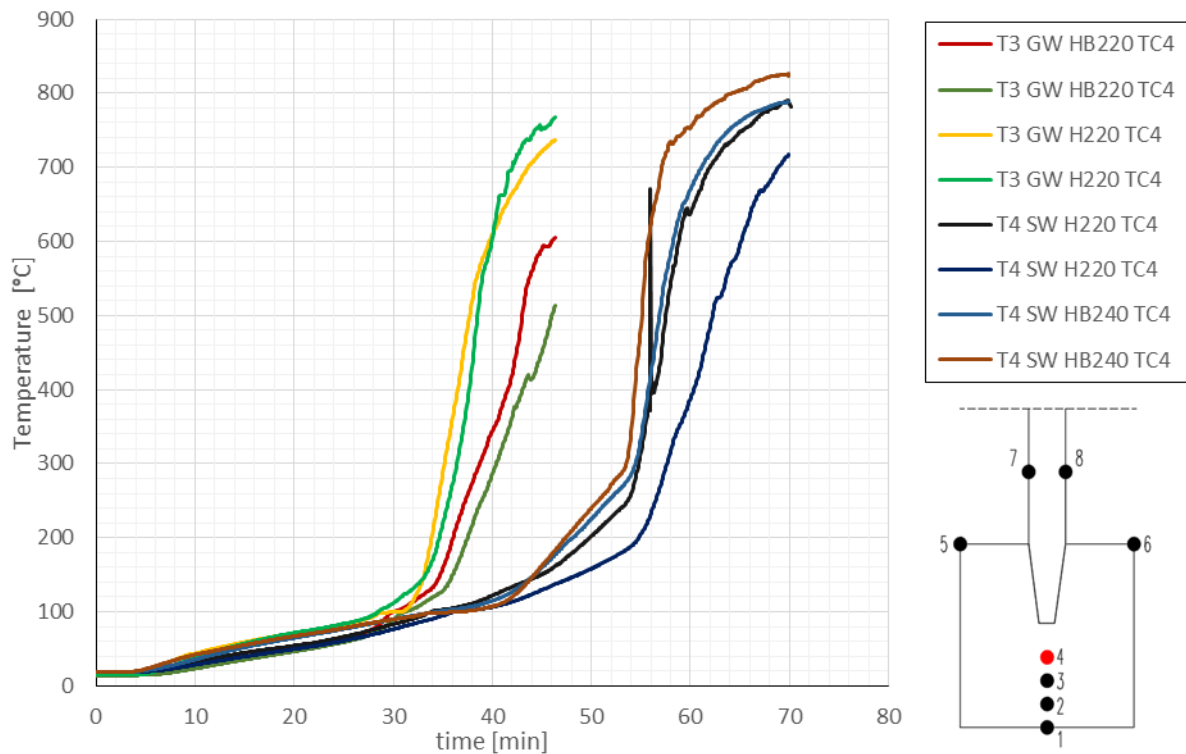


Figure 4.2-8 Thermocouple 4 (TC4) reading for I-beams tested in T3; T4

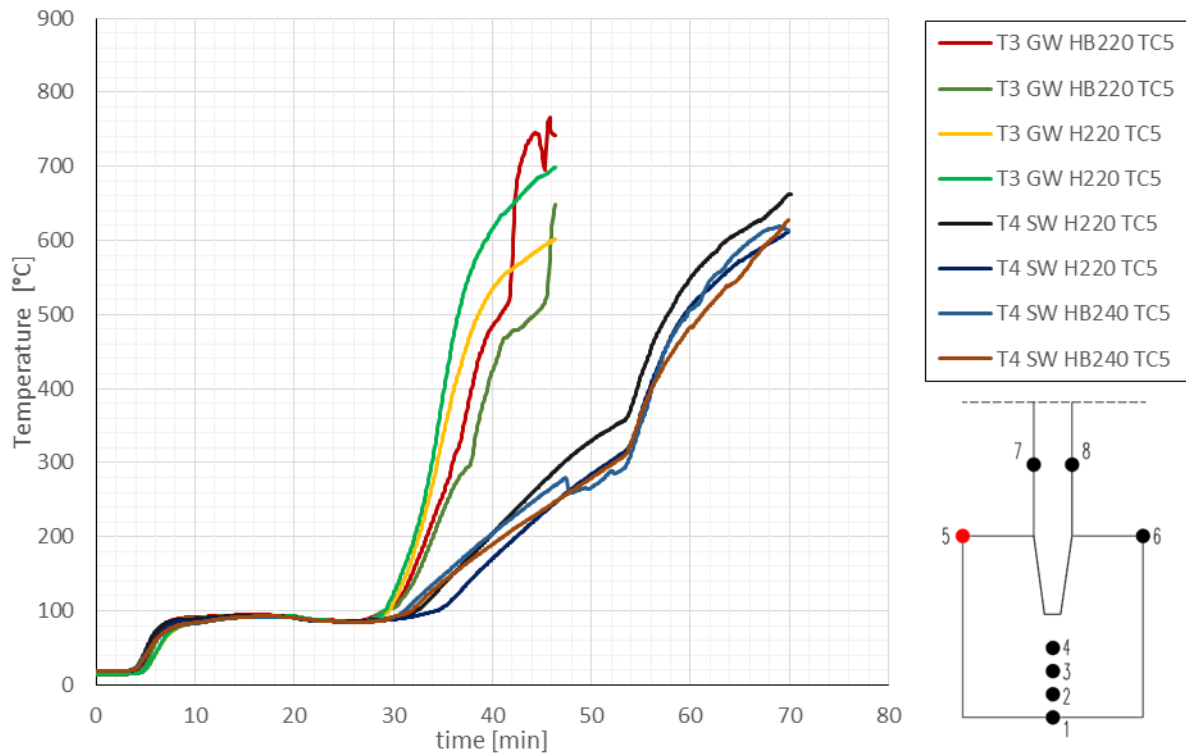


Figure 4.2-9 Thermocouple 5 (TC5) reading for I-beams tested in T3; T4

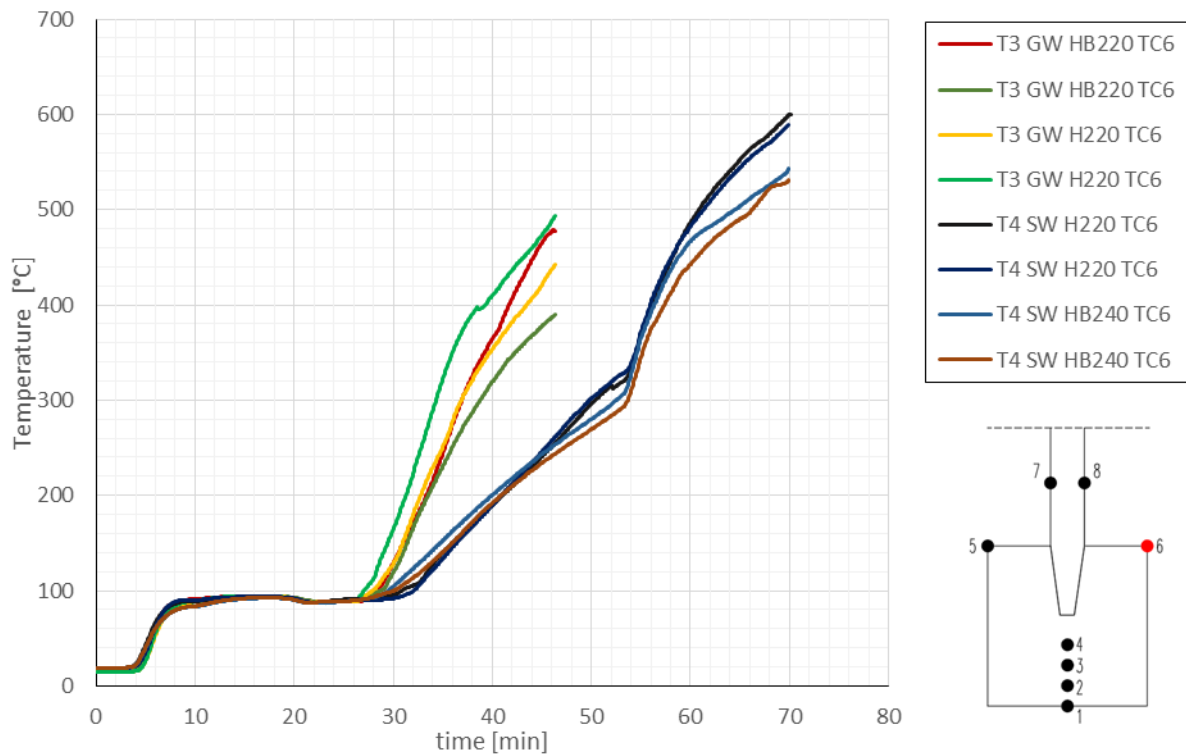


Figure 4.2-10 Thermocouple 6 (TC6) reading for I-beams tested in T3; T4

5 Analysis

5.1 Start time of charring and fall-off times

The start time of charring is registered when the thermocouple on the surface of the lower flange reaches 300°C and the failure of the gypsum board is when that same thermocouple records a sudden rise in temperature as a result of a protective gypsum board failing and the thermocouple exposed to the full heat of the furnace. The start time of charring and the failure time of the gypsum board is given in Table 5-1.

Table 5-1 Start times of charring and failure times

	Beam	Start time of charring [min]	Failure time of the gypsum board [min]
Test 1	T1 SW H200	22,1	26,0
	T1 SW HI200	20,7	26,0
	T1 SW LVL200	23,0	26,0
	T1 SW H200	28,0	33,0
	T1 SW HI200	25,4	33,0
	T1 SW LVL200	24,9	33,0
Test 2	T2 VOID H200	25,3	25,3
	T2 VOID HI200	23,4	25,3
	T2 VOID LVL200	25,5	25,3
	T2 GW H200	27,9	33,2
	T2 GW HI200	28,1	33,2
	T2 GW LVL200	30,3	33,2
Test 3	T3 GW H220	25,7	26,0
	T3 GW H220	25,7	26,0
	T3 GW HB240	25,8	26,0
	T3 GW HB240	25,8	26,0
Test 4	T4 SW H220	29,3	53,0
	T4 SW H220	29,4	53,0
	T4 SW HB240	30,2	53,0
	T4 SW HB240	29,0	53,0

5.2 Charring rate

The charring rate in the middle of the flange width (β_m) is measured by thermocouples during the test. The temperature for charring is regarded as 300°C. Charring of the I-joists in the vertical axle of the cross-section are found in Figure 5.2-1 and Figure 5.2-2. Charring rate is graphed using thermocouples 1 to 4 and time when they reached 300°C.

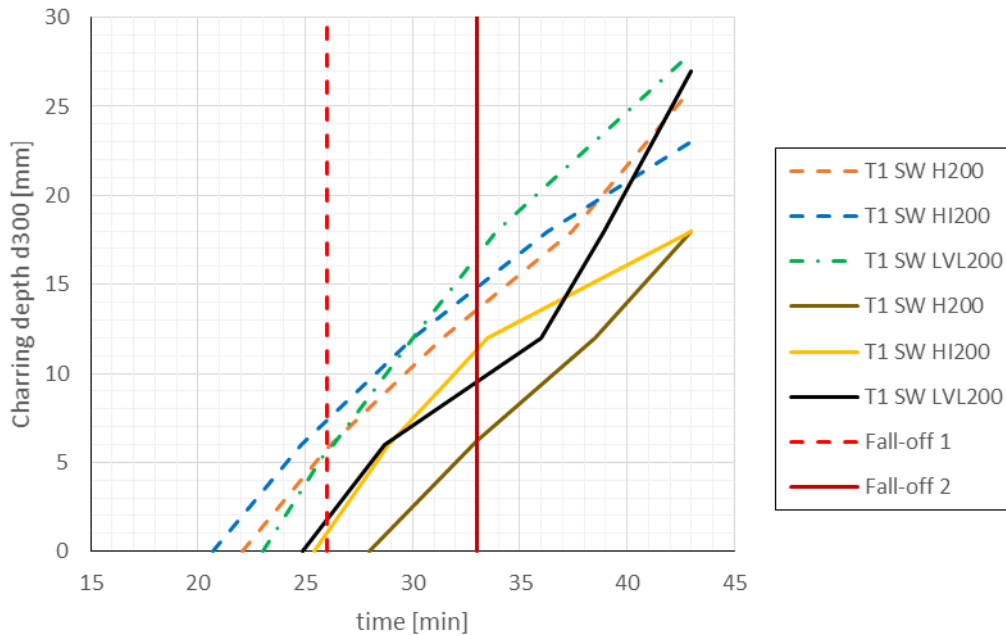


Figure 5.2-1. Charring of the beams in the middle of the flange for test 1

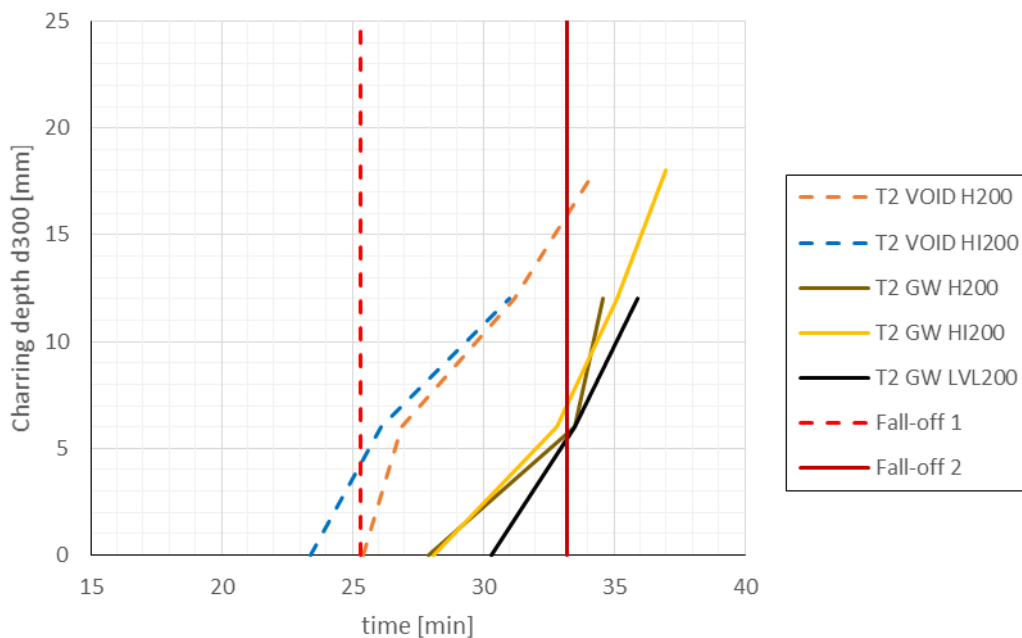


Figure 5.2-2. Charring of the beams in the middle of the flange for test 2

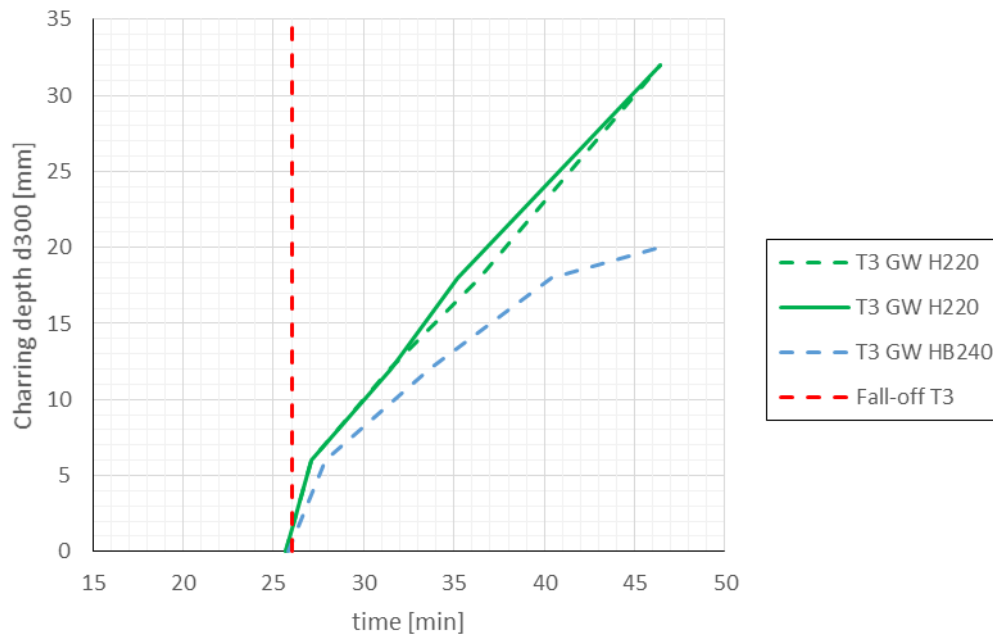


Figure 5.2-3 Charring of the beams in the middle of the flange for T3

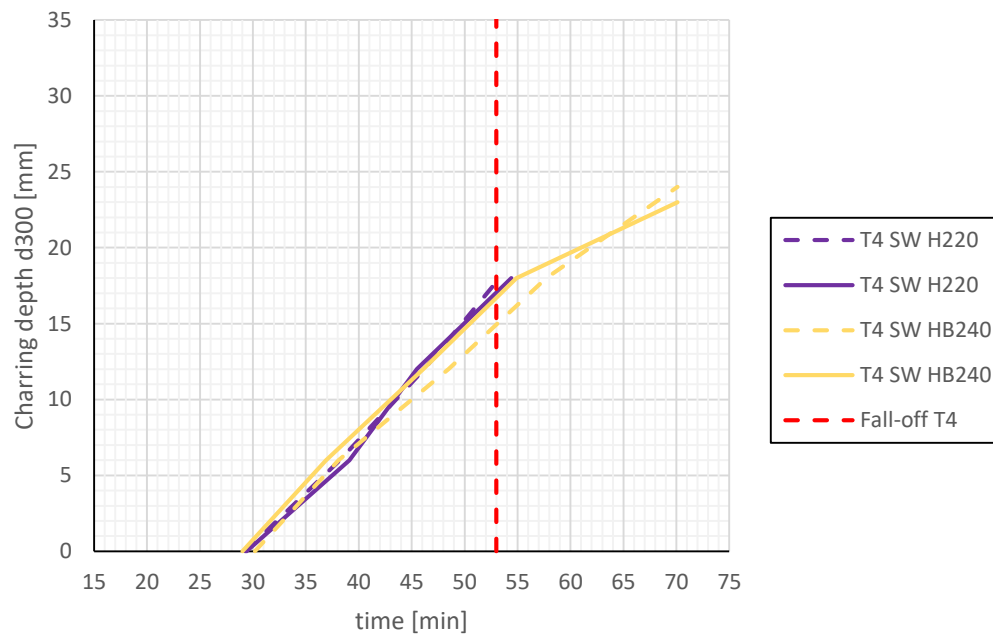


Figure 5.2-4 Charring of the beams in the middle of the flange for T4

Equation (17) and (18) were used to determine the values for charring rates in the protection and the post-protection phase. The values are presented in Table 5-2.

$$\beta_2 = \frac{d_2 - d_1}{t_f - t_{ch}} \quad (12)$$

Where β_2 is the charring rate in the protection phase d_2 is charring depth in terms of t_f , d_1 is the charring depth in terms of t_{ch} , t_f is the failure time of the cladding, t_{ch} is the start time of charring.

$$\beta_3 = \frac{d_3 - d_2}{t - t_f} \quad (13)$$

Where β_3 is the charring rate in the post-protection phase, d_3 is charring depth in terms of t , t is the total test time.

Table 5-2 Charring rates

	Beam	Charring rate in protection phase [mm/min]	Charring rate in post-protection phase [mm/min]
Test 1	T1 SW H200	1,48	1,08
	T1 SW HI200	1,41	1,02
	T1 SW LVL200	1,91	1,57
	T1 SW H200	1,25	1,17
	T1 SW HI200	1,71	0,94
	T1 SW LVL200	1,58	1,43
Test 2	T2 VOID H200	-	1.88
	T2 VOID HI200	2,71	1,21
	T2 VOID LVL200	-	-
	T2 GW H200	0,89	5,27
	T2 GW HI200	1,34	4,19
	T2 GW LVL200	1,84	3,54
Test 3	T3 GW H220	-	1,34
	T3 GW H220	-	1,35
	T3 GW HB240	-	0,74
	T3 GW HB240	-	0,74
Test 4	T4 SW H220	0,75	-
	T4 SW H220	0,74	-
	T4 SW HB240	0,65	0,48
	T4 SW HB240	0,70	0,33

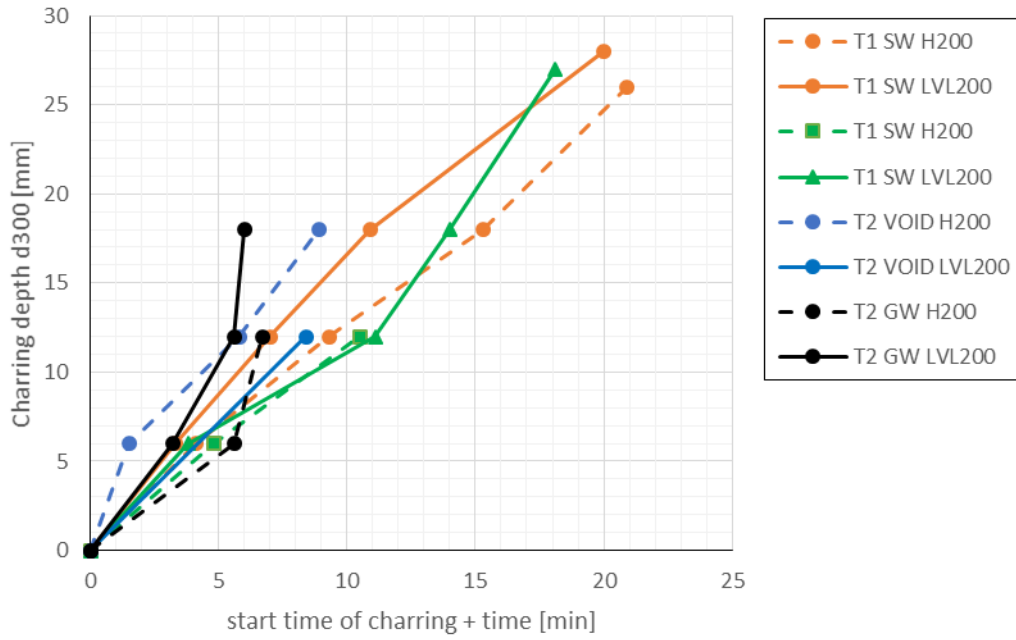


Figure 5.2-5 Comparison between charring of LVL and H

Some values for charring rates are missing as a result of $t_f = t_{ch}$. A few are caused by faulty thermocouples.

5.3 Recession speed

Recession speed is the rate at which cavity insulation disintegrates and can be evaluated from test results by using the following equation:

$$v_{rec} = \frac{d_{300}(t_{5,6})}{t_{5,6} - t_{ch}} \quad (14)$$

Where $d_{300}(t_{5,6})$ is the charring depth on the wood-insulation interface, $t_{5,6}$ is the average time of when thermocouple 5 and 6 registered 300°C.

Table 5-3 Start time of charring, recession speed

	Beam	Start time of charring [min]	Time when charring reaches 2/3 (T1,T2) or total flange height (T3,T4) [min]	Recession speed [mm/min]
Test 1	T1 SW H200	22,1	33,3	2,77
	T1 SW HI200	20,7	32,5	2,63
	T1 SW LVL200	23,0	29,9	4,49
	T1 SW H200	28,0	39,0	2,82
	T1 SW HI200	25,4	35,7	3,01
	T1 SW LVL200	24,9	37,8	2,40
Test 2	T2 VOID H200	25,3	27,7	12,92
	T2 VOID HI200	23,4	31,0	4,08
	T2 VOID LVL200	25,5	28,9	9,12
	T2 GW H200	27,9	31,7	8,16
	T2 GW HI200	28,1	30,9	11,07
	T2 GW LVL200	30,3	32,5	14,09
Test 3	T3 GW H220	25,7	34,2	5,6
	T3 GW H220	25,7	35,7	4,7
	T3 GW HB240	25,8	38,1	3,8
	T3 GW HB240	25,8	36,5	4,4
Test 4	T4 SW H220	29,3	53,1	2,0
	T4 SW H220	29,4	53,1	2,0
	T4 SW HB240	30,2	50,8	2,3
	T4 SW HB240	29,0	48,9	2,4

Recession speed can be shown as the slope of an ascending line where the start point of the line is start time of charring and end point is when the thermocouple on the lateral side of the flange registered 300°C.

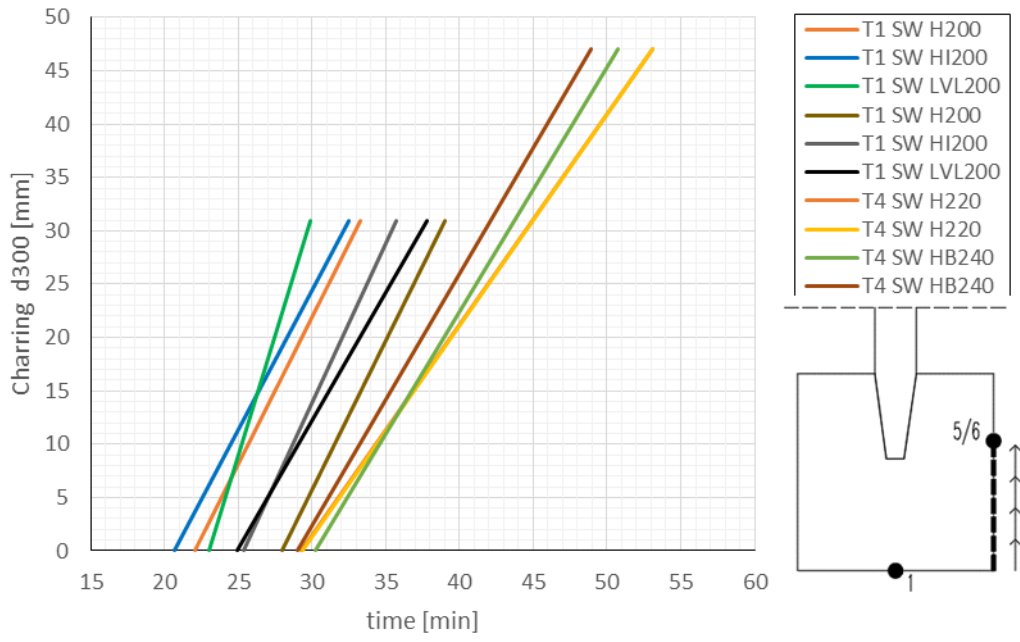


Figure 5.3-1 Charring on the wood-insulation interface; T1 and T4

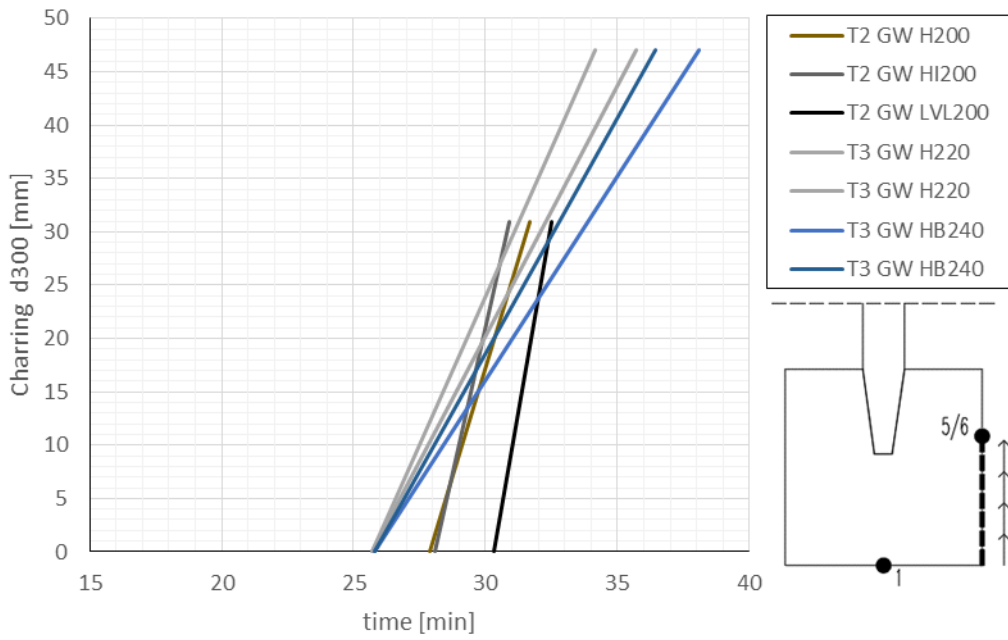


Figure 5.3-2 Charring on the wood-insulation interface; T2 and T3

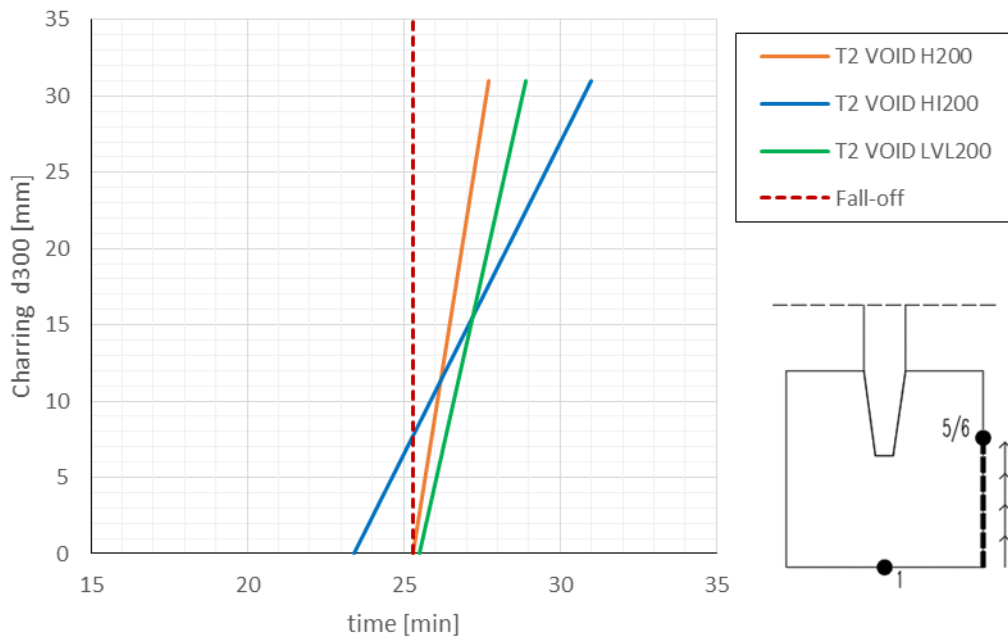


Figure 5.3-3 Charring on the wood-insulation interface; T2 VOID

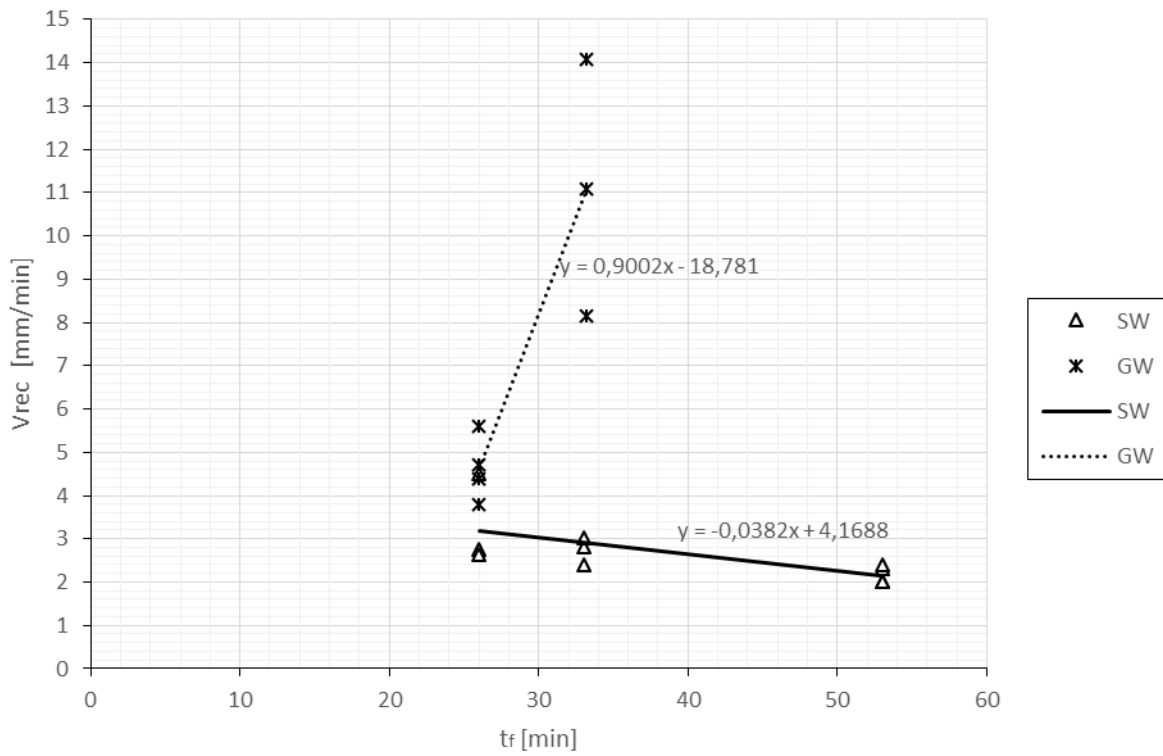


Figure 5.3-4 Recession speed for GW and SW

Recession speed for stone wool should be taken as $3 \text{ mm}/\text{min}$ to be conservative.

5.4 Residual cross-sections

After the test specimen is extinguished and cooled down. A section of the residual beam is cut off with a sabre saw and scrubbed with a steel brush – everything that is detaching from the wood is char and everything that remains is considered wood.

Table 5-4 Charring depths, remaining height of the flanges and area

	Beam	Height of the flange [mm]	Remaining height of the flange [mm]	Charring depth in the middle [mm]	Remaining flange area [mm ²]
Test 1	T1 SW H200	47	21	26	658,9
	T1 SW HI200	47	24	23	1291
	T1 SW LVL200	39	11	28	130,0
	T1 SW H200	47	31	16	1197,4
	T1 SW HI200	47	33	14	1735,1
	T1 SW LVL200	39	13	27	277,5
Test 2	T2 VOID H200	47	0	47	1166,0
	T2 VOID HI200	47	0	47	1976,2
	T2 VOID LVL200	39	0	39	600,9
	T2 GW H200	47	27	20	732,2
	T2 GW HI200	47	33	14	185,7
	T2 GW LVL200	39	25	14	672,2
Test 3	T3 GW H220	47	15	32	572,4
	T3 GW H220	47	15	32	614,3
	T3 GW HB240	47	27	20	2805,8
	T3 GW HB240	47	27	20	2892,5
Test 4	T4 SW H220	47	0	-	0
	T4 SW H220	47	0	-	0
	T4 SW HB240	47	23	24	1585,7
	T4 SW HB240	47	24	23	1628,8



Figure 5.4-1
T1 SW H200



Figure 5.4-2
T1 SW H200

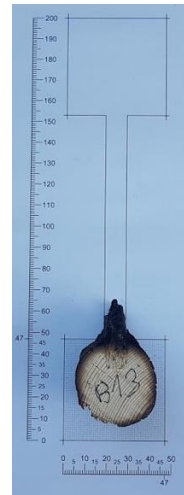


Figure 5.4-3
T2 VOID H200



Figure 5.4-4
T2 GW H200



Figure 5.4-5
T1 SW HI200



Figure 5.4-6
T1 SW HI200

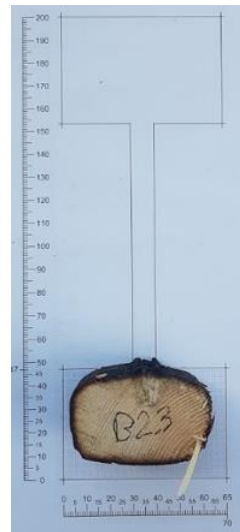


Figure 5.4-7
T2 VOID HI200



Figure 5.4-8
T2 GW HI200



Figure 5.4-9
T1 SW LVL200



Figure 5.4-10
T1 SW LVL200

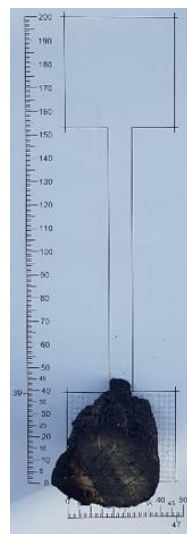


Figure 5.4-11
T2 VOID LVL200



Figure 5.4-12
T2 VOID GW200

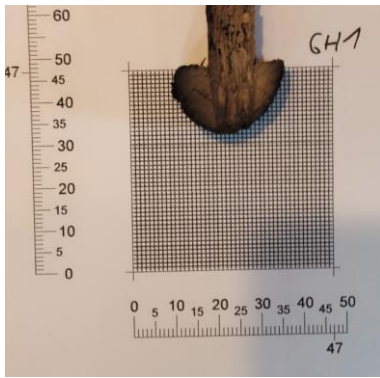


Figure 5.4-13
T3 GW H200

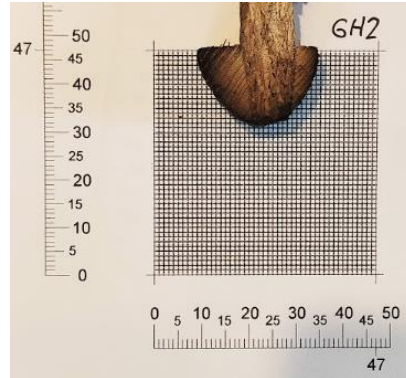


Figure 5.4-14
T3 GW H200

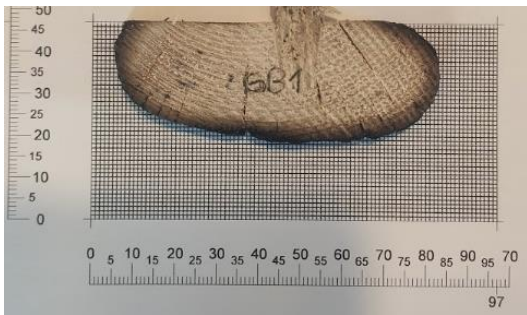


Figure 5.4-15
T3 GW HB240



Figure 5.4-16
T3 GW HB240

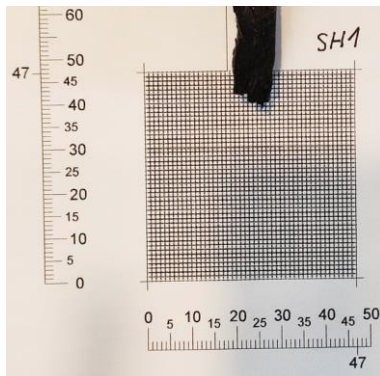


Figure 5.4-17
T4 SW H200

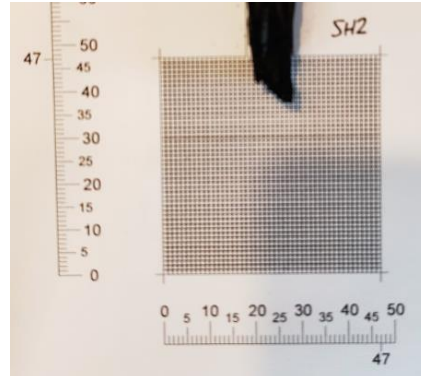


Figure 5.4-18
T4 SW H200

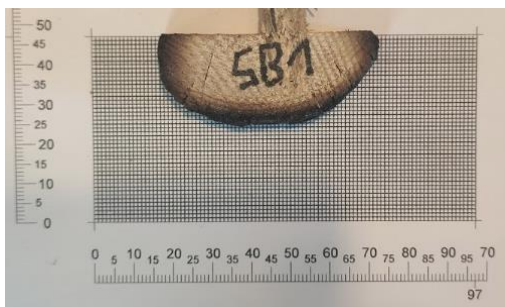


Figure 5.4-19
T4 SW HB240

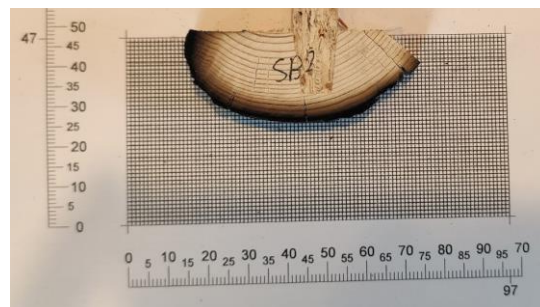


Figure 5.4-20
T4 SW HB240

5.5 Cross-section factor

Cross-section factor k_s takes into account that narrower members have an increased charring rate. The precise values for the cross-section factor was derived using equation (15). The values are presented in Table 5-5.

$$k_s = \frac{d_{char,protection}}{\beta_0 * k_2 * (t_f - t_{ch})} \quad (15)$$

Due to no protection phase and thermocouple malfunction there are no evaluation for beam T2 GW HI200.

Table 5-5 Evaluated cross-section factors

Member	Flange width [mm]	Evaluated k_s
T1 SW H200	47	3,12
T1 SW HI200	47	2,62
T1 SW H200	47	1,87
T1 SW HI200	70	2,94
T1 SW LVL200	70	3,15
T2 GW H200	47	2,48
T2 GW HI200	47	-
T4 SW H220	47	1,58
T4 SW H220	47	1,53
T4 SW HB240	97	1,38
T4 SW HB240	97	1,46

The cross-section factor takes into account that narrower timber members experience a faster rate of charring. Figure 5.5-1 presents trendlines for evaluated cross-sections factors for each test. Trendline that takes into account every test is marked as "Total". Trendline for cross-section factor is ascending, which means that wider members have a lower value for the cross-section factor and experience a slower rate of charring than narrower members.

König 2005 is calculated according to the following equation:

$$k_{b,ch} = k_s = \frac{27,4}{b} + 1 \quad (16)$$

Where b is width of the beam. [18]

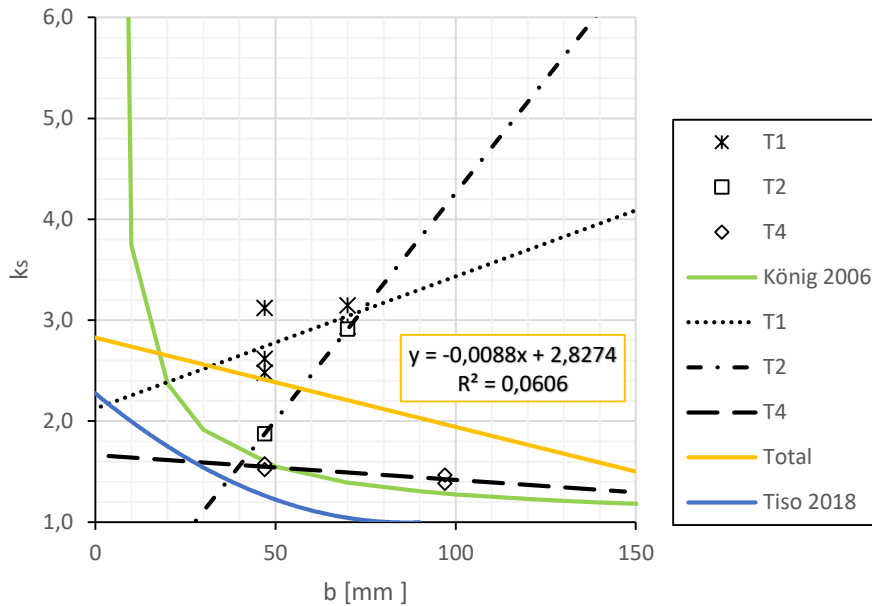


Figure 5.5-1 Evaluated cross-section factors.

It is plausible that the gypsum board did not offer full protection for T1 and T2 and the heat infiltrated specimens before the failure of the cladding. Therefore no definite line between protection and post-protection phase could be drawn as both phases blended together.

Figure 5.5-1 shows that total trendline is descending. This indicates that test results are consistent with the theory that charring rate decreases as the width of the cross-section increases.

An expression to determine the values for k_s as a function of the width of the I-beams is shown below:

$$k_s = 2,83 - 0,0088b \quad (17)$$

In Table 5-6 cross-section factor k_s values are given for each type of I-joists that were tested. The values are calculated using the equation (17) above.

Table 5-6 Cross-section k_s values for tested beams using equation (17)

Flange width [mm]	Evaluated k_s
47	2,41
70	2,21
97	1,97

5.6 Post-protection factor

Post-protection factor k_3 is a protection factor for charring phase 3 (see Figure 2.6-1 for phases) and it takes into account that charring increases after the failure of the gypsum board. The precise values for the cross-section factor was derived using equation (19).

$$k_3 = \frac{d_{char,post-protection}}{\beta_0 * k_s * (t - t_f)} \quad (18)$$

where $d_{char,post-protection}$ is charring that occurred during phase 3, β_0 is the basic design charring rate. k_s is the cross-section factor t is the duration of the test and t_f is fall-off time of the gypsum board.

The values for k_s for glass wool have been calculated using equation (18). Evaluated post-protection factors are presented in Table 5-7

Table 5-7 Evaluated post-protection factors k_3 for glass wool

Member	Evaluated k_3
T2 GW H220	2,49
T2 GW HI220	2,01
T2 GW LVL200	1,81
T3 GW H220	1,10
T3 GW H220	1,24
T3 GW HB240	0,97
T3 GW HB240	1,09

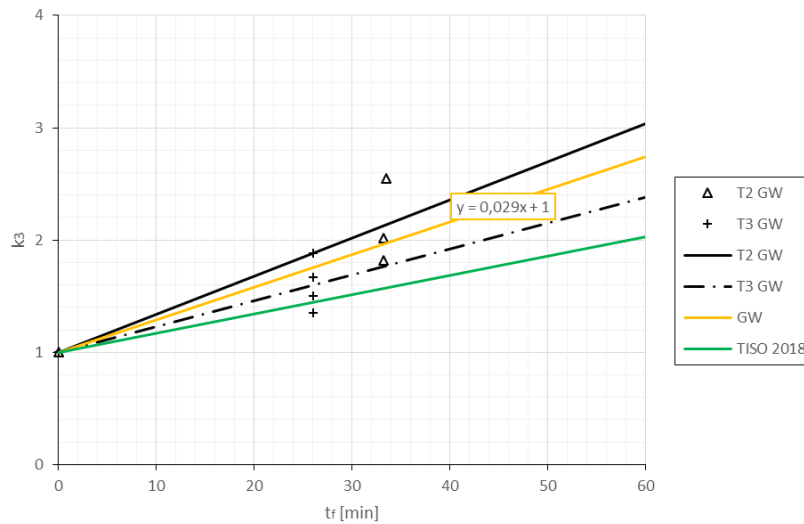


Figure 5.6-1 Protection factor for glass wool

Post-protection factor for I-joists in timber frame assemblies with glass wool as cavity insulation should be expressed as:

$$k_3 = 1 + 0,029t_f \quad (19)$$

The values for k_3 for stone wool have been calculated using equation (18). Evaluated post-protection factors are presented in Table 5-8.

Table 5-8 Evaluated post-protection factors k_3 for stone wool

Member	Evaluated k_3
T1 SW H200	0,76
T1 SW HI200	0,64
T1 SW LVL200	0,83
T1 SW H200	0,37
T1 SW HI200	0,46
T1 SW LVL200	1,11

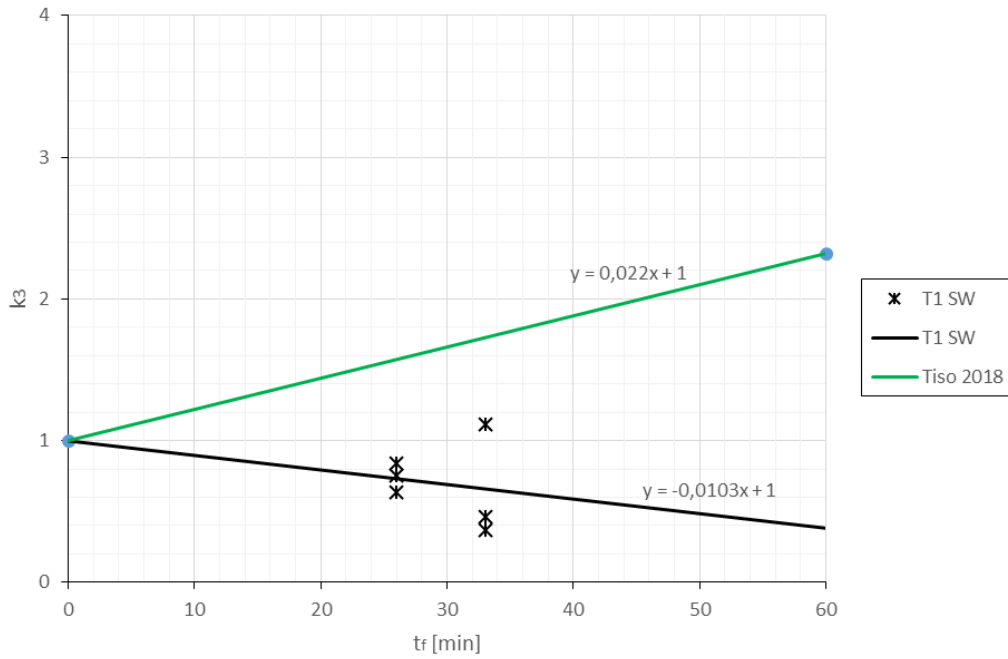


Figure 5.6-2 Protection level for stone wool

Test results are the opposite to the theory and show that charring rate is decreasing after the failure of the cladding. Current test results are based only on T1 and it is plausible that gypsum board did not offer full protection in phase 2. No charring took place in phase 3 for T4. More research is needed for I-joists with stone wool as cavity insulation.

6 Comparison

Figure 5.6-1 to Figure 5.6-6 show a comparison in charring rates from fire tests and theoretical charring rates. Theoretical values have been calculated in two ways:

1. Using design values for dimensional lumber with rectangular cross-section. The cross-section factor k_s has been evaluated using equation (8) and post-protection factors using equation (9) and (10). „Calculation results (rectangular)“ on the graphs.
2. Using the design values proposed in the framework of this thesis. The cross-section factor k_s has been evaluated using equation (17). The post-protection factor for glass wool was evaluated using equation (19). The post-protection factor for stone wool was evaluated using equation (10)

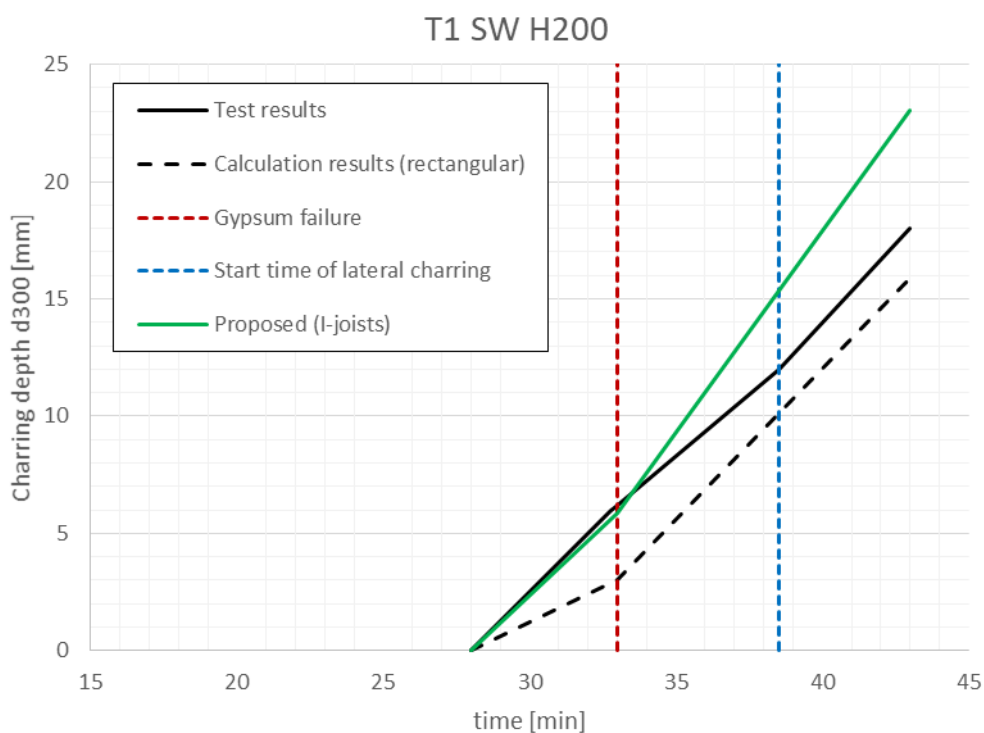


Figure 5.6-1 Comparison for T1 SW H200

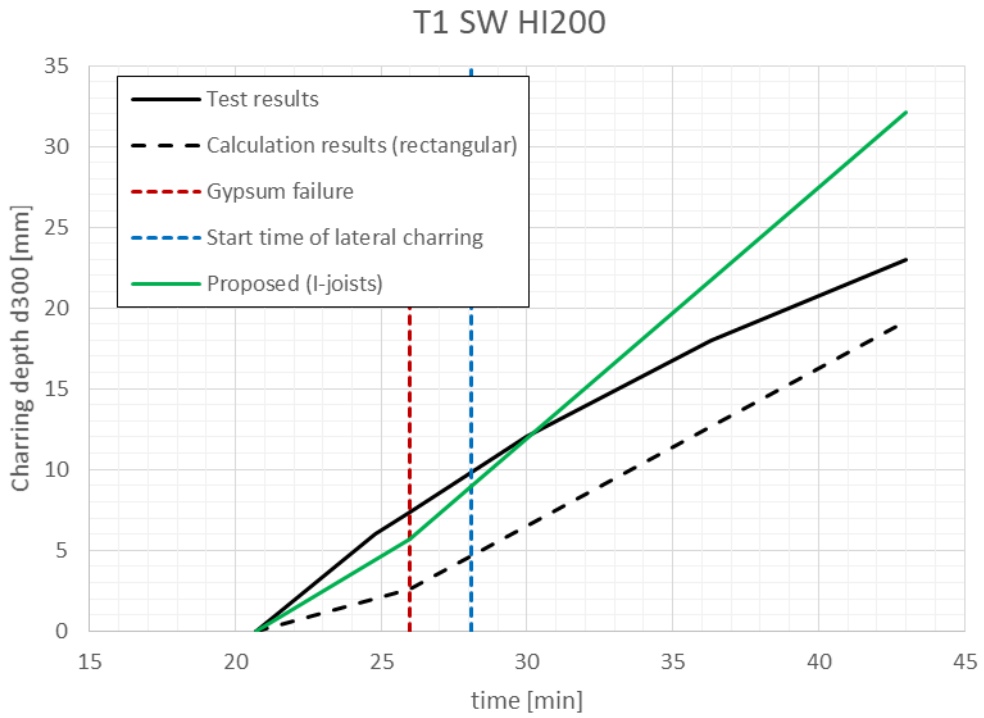


Figure 5.6-2 Comparison for T1 SW HI200

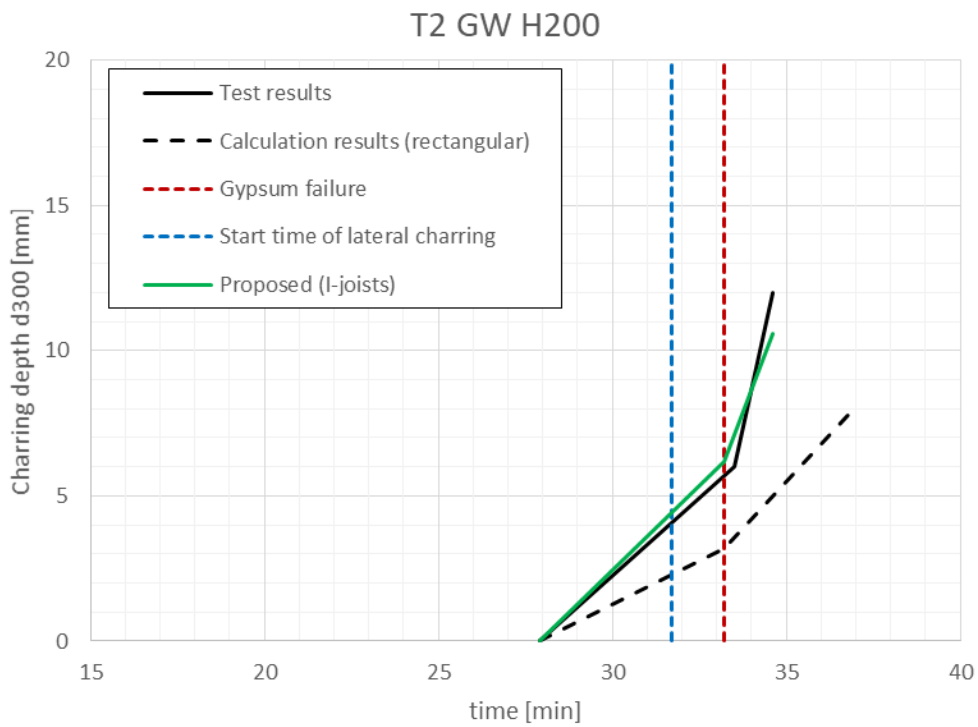


Figure 5.6-3 Comparison for T2 GW H200

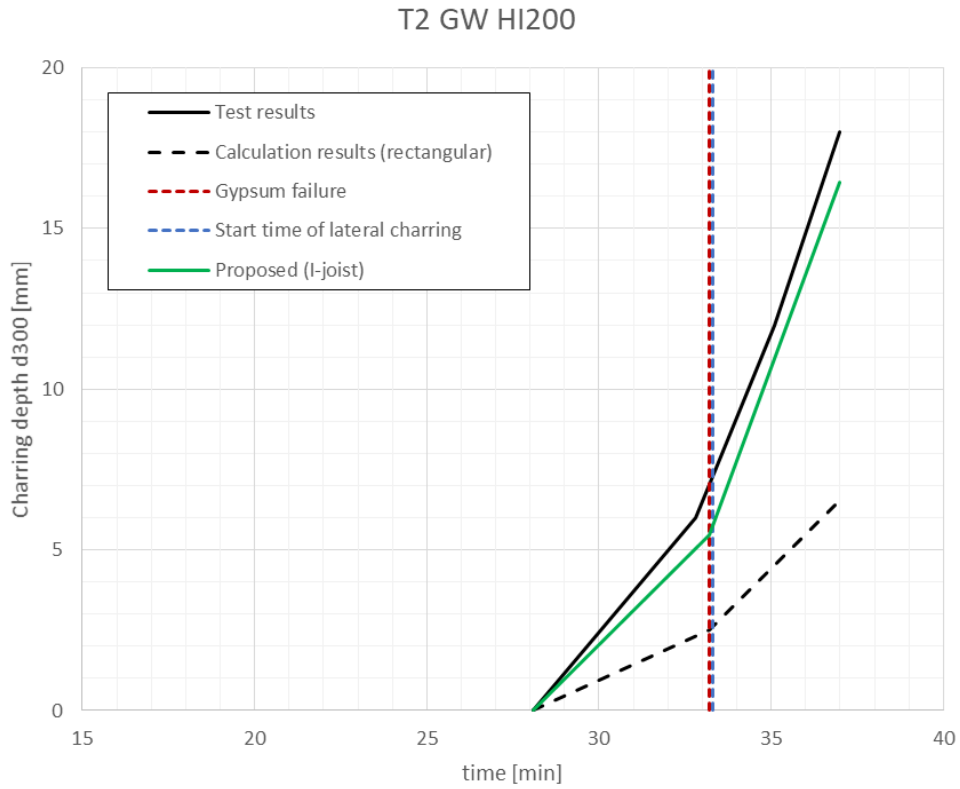


Figure 5.6-4 Comparison for T2 GW HI200

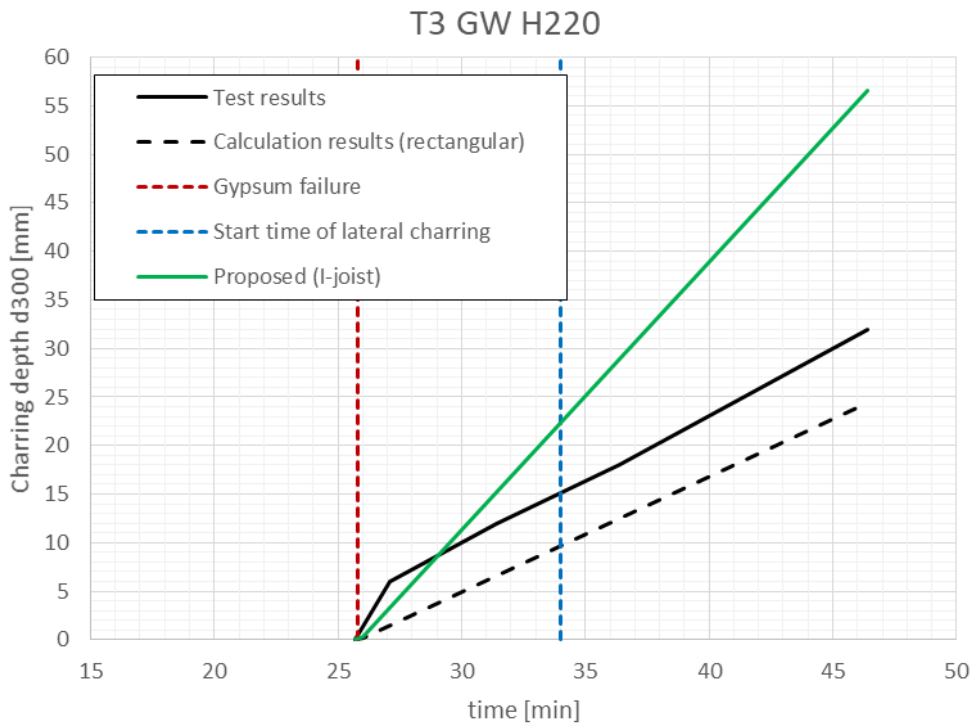


Figure 5.6-5 Comparison for T3 GW H220

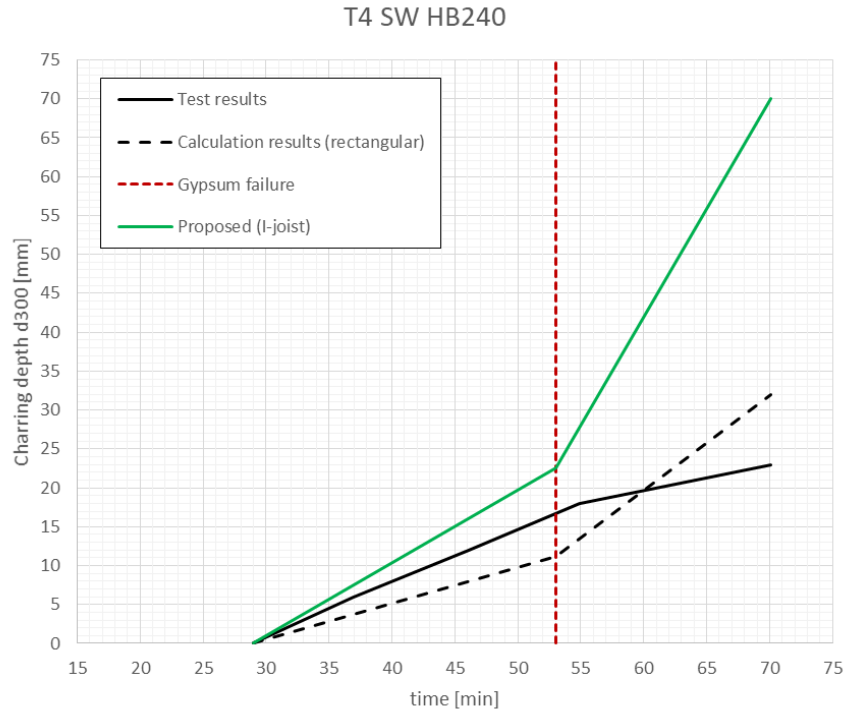


Figure 5.6-6 Comparison for T4 SW HB240

The obtained equations mostly yield results that can be considered safe when compared to actual fire tests. This implies that charring depth is as deep or deeper than fire tests. However, since the proposed equations are based on average values then in some cases theoretical charring depth is not as deep as in fire tests. Also, the theoretical start time of charring and failure time of the cladding have been set equal to those times experienced in the fire test. In practice, those times are calculated and provide even safer results.

7 Conclusion

As engineered wooden I-joists become more popular in framing then more information is needed on the topic of fire safety. Currently there is no information about I-joists in Eurocode 5 Part 1-2.

The aim of this thesis was to develop equations and find values for factors that are used for finding charring depth. A total of 4 model scale fire tests were conducted for this thesis. I-beams in those tests were exposed to the standard temperature-time fire curve (ISO 834). Each test was a timber frame assembly with stone wool, glass wool, or nothing as cavity insulation. Type F gypsum board was used for the cladding. Overall 16 I-joists were investigated.

A number of thermocouples were installed for each I-beam to determine the failure of the cladding, start time of charring, and charring rate. After the tests, a sample was cut from each I-beam and residual cross-sections registered.

From the analysis of the 4 fire tests, the following conclusions could be drawn for I-joists charring behaviour:

1. Wooden I-joists are subjected to a faster rate of charring than compared to the dimensional wood with rectangular cross-sections. A new design equation for the cross-section factor k_s is provided from the fire tests conducted. The cross-section value is related to the width of the beam.
2. A new equation is given for the post-protection factor k_3 for I-joists in timber frame assemblies with glass wool as cavity insulation. The equation is a function of the fall-off time of the cladding.

The obtained equations are based off on 4 fire tests. Further research and more data are needed to propose equations that are fit for the European Standard.

8 Resümee

Puitu on sajandeid kasutatud ehitusmaterjalina. Puit on tänu heale kättesaadavusele, töödeldavusele ning montaaži lihtsusele enam levinud väiksemate hoonete ja rajatiste ehitamisel. Samas on viimase sajandi jooksul puitu järjest enam asendatud uuemate materjalidega: teras, betoon, kergbetoon jms. Üheks põhjuseks, miks puitu vähem kasutatakse, on karmistunud tuleleohutusnõuded. Puitu peetakse kergesti süttivaks, kuigi selle süttimiseks on vajalik kas otsene leek või väga kõrge temperatuur. Puit ehitusmaterjalina on keskkonnasõbralik ja taastuv materjal, kuid ehitussektoris veel siiski alahinnatud. Piisavate meetmete rakendamisel on puit arvestatav ehitusmaterjal.

Puidu kasutusvõimalused ehitussektoris üha laienevad, sest puidutehnoloogia areng on väga kiire. Üheks näiteks on I-talade kasutuselevõtt. Võrreldes tavalise saepuiduga on I-alad on kergemad ja kvaliteetsemad. Puit I-talad koosnevad kolmest osast: ülemine vöö, alumine vöö ning vöösid omavahel ühendavast seinast. I-tala sein on tavaliselt valmistatud OSB-st või vineerist ning vööd on täispuidust või lamineeritud saematerjalist (LVL). I-talaid on võimalik teha kuni 18 meetri pikkusega kuna talaid saam oma vahel sõrmühendada.

I-talad on muutunud ehituses laialdaselt kasutatavaks nii põrandate, katuste kui seinte ehituskonstruktsioonides. Tänu tugevuse ja väiksemale kaalule asendavad nad järk-järgult traditsioonilist saematerjali. Lisaks on I-talad konstrueeritud arvestades rangeid kvaliteedinõudeid ning nende niiskusesisaldus on madal, vähendades seeläbi kokkukuivamise mõjusid. I-talaid on nende kaalu tõttu lihtne transportida ja ehitusel paigaldada.

I-taladest valmistatud konstruktsioonid on otsese tule suhtes tundlikumad, sest need põlevad kiiremini ja kaotavad otsese tulega kokkupuutel oma konstruktsiooni terviklikkuse rutem kui samade mõõtmetega saematerjalist konstruktsioonid. Seetõttu on oluline aru saada kuidas tuli mõjutab I-talaid, et projekteerijatel oleks usaldusväärsed juhised turvaliste ehitiste projekteerimisel.

Lõputöö eesmärk

Antud magistritöö peamine eesmärk on välja töötada projekteermismeetod I-talade söestumissügavuse leidmiseks standardtulekahjuolukorras. Selles lõputöös tehtavate katsete põhjal pakutakse välja söestumistegurite leidmise meetod

9 References

- [1] "Regulation (EU) No 305/2011 of the European Parliament and of the Council," Official Journal of the European Union, Brussels, 2011.
- [2] "Application and use of eurocodes," European Commission, Brussels, 2003.
- [3] B. Östman and B. Källsner, "National building regulations in relation to," Växjö University, Sweden, 2011.
- [4] EN 1995-1-2:2004 Eurocode 5., " "Design of timber structures – Part 1-2: General – Structural fire design European Standard.," European Committee for Standardization, Brussels.
- [5] EN 13501-2:2009, "Fire classification of construction products and building elements – Part 2: Classification using data from fire resistance tests, excluding ventilation services.," European Committee for Standardization, Brussels.
- [6] Fire safety in timber buildings – Technical guideline for Europe, Stockholm: SP Technical Research Institute of Sweden, 2010.
- [7] H. J. Blass, P. Aune, B. Choo and R. G. Görlacher, Timber Engineering STEP 1, Centrum Hout, 1995.
- [8] R. T. Bynum, Insulation Handbook, McGraw-Hill Professional, 2001.
- [9] "EN 1991-1-2:2002. Eurocode 1 : Action on Structures – Part 1-2: General actions - Actions on structures exposed to fire.," European Standard. European, Brussels.
- [10] A. Just, J. Schmid and J. König, "Gypsum plasterboards used as fire protection," SP Technical Research Institute of Sweden, Stockholm, 2010.
- [11] M. Tiso, "The Contribution of Cavity Insulations to the Load-Bearing Capacity of Timber Frame Assemblies Exposed to Fire," TTÜ press, Tallinn, 2018.
- [12] prEN ISO 9229 , "Thermal insulation - Definitions of terms. European Standard.," CEN/TC88, Brussels, 2006.
- [13] A. Just, " Post-protection behaviour of wooden wall and floor structures completely filled with glass wool, SP Report 2010:28," SP Technical Research Institute of Sweden, Stockholm, 2010.
- [14] J. König and L. Walleij, "One-dimensional charring of timber exposed to standard and parametric fires in initially unprotected and postprotection situations," Träteck, Stockholm, 1999.
- [15] J. König and L. Walleij, "Timber frame assemblies exposed to standard and parametric fires. Part 2: A design model for standard fire exposure.," Träteck, Swedish Institute for Wood Technology Research, Report No. 0001001, Stockholm , 2000.
- [16] E. Allen and J. Iano, ". Fundamentals of Building Construction," John Wiley & Sons Inc, Hoboken, 2004.

- [17] L. Koel, "Carpentry, 4th Edition," Thompson Delmar Learning, Clifton Park, NY, 2001.
- [18] K. J., "Fire exposed simply supported wooden I-joists in floor assemblies. SP report 2006;44," SP Swedish National Testing and Research Institute, Stockholm, 2006.
- [19] D. J. Hopkin, "The Fire Performance of Engineered Timber," Loughborough University, Leicestershire, 2011.
- [20] ISO 834-1:1999 , "Fire-resistance tests — Elements of building construction — Part 1: General requirements," International Organization for Standardization.
- [21] EN 520:2004+A1:2009, " Gypsum plasterboards - Definitions, requirements and test methods.," European Committee for Standardization, Brussels.
- [22] EN 1363-1 , "Fire resistance tests - Part 1: General requirements," European Committee for Standardization, Brussels..
- [23] A.Just, E.Just and K. Õiger, Puitkonstruktsioonide erikursus, Tallinn: Tallinna Tehnikaülikool, 2013.